
**The Role of Polo-like Kinase 1 (PLK1) in
Homologous Recombination During Mammalian
Spermatogenesis**

by

Xueqi Zhao

A dissertation submitted to Johns Hopkins University in conformity with the
requirements for the degree of Master of Science

Baltimore, Maryland

April 2018

© Xueqi Zhao 2018

All rights reserved

ABSTRACT

Failure in accurate segregation of chromosomes during meiosis causes aneuploidy, the main contributor to infertility, spontaneous abortions, and developmental defects. A molecular understanding of the factors that regulate chromosome dynamics during meiosis is necessary to better understand the cellular origins of these aneuploidy events. Polo-like kinase 1 (PLK1) participates in processes during the cell cycle, such as DNA replication, mitotic entry, chromosome segregation and cytokinesis. In this study, we focused our attention on the role of PLK1 during a DNA damage repair event, homologous recombination. Previous studies have shown that PLK1 has a central role in regulating an early recombination intermediate, RAD51, as well as in influencing Class II MUS81-EME1 crossover pathway. We used a germ-cell-specific conditional knockout strategy, driven by *Spo11-Cre* recombinase, to assess the role of PLK1 in regulating the transition from prophase to metaphase in mouse spermatocytes.

Our results showed *Plk1* conditional knockout mice were infertile and displayed severe meiotic aberrancies, including enlarged primary spermatocytes and increased apoptotic cells. Interestingly, we observed alterations in recombination protein foci numbers occurring during homologous recombination. These results underscore the importance in maintaining strict temporal control of PLK1 activity during spermatogenesis.

Advisor: Dr. Philip Jordan, Department of Biochemistry and Molecular Biology, Johns Hopkins University Bloomberg School of Public Health

Secondary reader: Dr. Michael J. Matunis, Department of Biochemistry and Molecular Biology, Johns Hopkins University Bloomberg School of Public Health

ACKNOWLEDGEMENTS

I would like to express my great gratitude to my ScM advisor, Philip Jordan for his patient guidance, enthusiastic encouragement and valuable suggestions during the development of this thesis work. I would also like to thank Steve Wellard for his assistance of technique and skill required to collect my data. My appreciation also goes to all remaining lab members in the Jordan Lab: Dr. Marina Pryzhkova, Grace Hwang, Jessica Hopkins, Tara Biser, Alisa Boyko, Maria Laura Reategui, Michelle Xu. Special appreciation is given to my thesis reader, Michael J. Matunis for his time and effort.

I would like to thank the entire faculty and staff of the department of Biochemistry and Molecular Biology for their effort to provide the resources for learning.

Finally, I would like to give my deep gratitude to my parents, who always support and encourage me throughout my study.

CONTENTS

ABSTRACT	ii
ACKNOWLEDGEMENTS	iv
CONTENTS	v
LIST OF TABLES	vi
LIST OF FIGURES	vii
INTRODUCTION	1
MATERIALS AND METHODS	13
RESULTS	19
DISCUSSION	35
PUBLIC HEALTH RELEVANCE	40
REFERENCES	42
CURRICULUM VITAE	47

LIST OF TABLES

TABLE 1. PCR set up for one sample	14
TABLE 2. Primers used in this study	14
TABLE 3. Krebs-Ringer bicarbonate solution (KRB)	16
TABLE 4. 0.1M sucrose solution, pH to ~8.0	16
TABLE 5. 1% Paraformaldehyde (PFA), pH to ~8.0	16
TABLE 6. Antibody Dilution Buffer (ADB)	17
TABLE 7. Hypotonic buffer	17
TABLE 8. Primary antibodies used in this study	18

LIST OF FIGURES

FIGURE 1. Overview of meiotic cell cycle	9
FIGUER 2. Overview of meiosis prophase I	10
FIGUER 3. Overview of homologous recombination	11
FIGUER 4. Introduction to Polo-like kinases	12
FIGUER 5. Relative testis weight and sterility	21
FIGUER 6. TUNEL stained cross-section	22
FIGUER 7. Hematoxylin and eosin stained cross-section	23
FIGUER 8. IHO1 chromatin spreads	25
FIGUER 9. RAD51 chromatin spreads	28
FIGUER 10. DMC1 chromatin spreads	29
FIGUER 11. MLH1 chromatin spreads	31
FIGUER 12. Cytological interference	32
FIGUER 13. CDK2 chromatin spreads	34
FIGUER 14. Proposed model for crossover recombination pathway	39

INTRODUCTION

Overview of meiosis prophase I and homologous recombination

Meiosis is an essential cell cycle stage required by all reproducing mammals for gametogenesis, which involves one round of DNA replication and two rounds of cell division to ultimately generate four haploid gametes (Fig. 1) (Handel & Schimenti, 2010). After completing chromosome replication in pre-meiotic S phase, a primary germ cell undergoes homologous chromosome synapsis during meiosis prophase I. Chromosome synapsis is the pairing of homologous chromosome via a zipper-like protein structure called the synaptonemal complex (SC) (Zickler and Kleckner, 1999). The SC is made up of lateral elements and central elements. Lateral elements, consist of SYCP2, SCYP3 and cohesins, and hold each pair of sister chromatids together. Homologous chromosome pairs are synapsed by bridging the lateral elements via central region proteins. The central region of the SC contains transverse filament, SYCP1, and central elements, SYCE1/2/3, and TEX12 (Costa et al., 2007; Fraune et al., 2012). The assembly and disassembly of the SC divide meiosis prophase I into five substages, defined as leptotema, zygotema, pachytene, diplotema and diakinesis (Fig. 2). At leptotema, SYCP2 and SYCP3 form axial elements between each pair of sister chromatids, with cohesins underlying framework for axial element formation (Fraune et al., 2012). By zygotema, central elements start to form between homologous chromosomes. At the pachytene stage, the SC is fully assembled along the axis of homologous chromosomes. By diplotema, central elements

start to dissociate but remain at the centromere. At diakinesis, lateral elements begin to disassemble but persist at the centromere until metaphase I (Cahoon & Hawley, 2016).

During meiotic prophase, homologous recombination (HR) is programmed to ensure physical association between homologous chromosomes, which ensures accurate chromosome segregation during meiosis (Fig. 3). HR initiates with double-strand breaks (DSBs) and differentiates into crossover and non-crossover pathways, also known as the double-strand break repair (DSBR) model and the synthesis-dependent strand annealing (SDSA) model (Szostak et al., 1983; McMahill et al., 2007). Crossover pathways go on to form double-Holliday junctions (dHJs) and ultimately generate a physical connection, known as chiasmata, which is crucial for bipolar attachment and proper segregation of maternal and paternal chromosomes at the first division of meiosis I (Roeder, 1997; Hirose et al., 2011). It is proposed that the choice of crossover over non-crossover is not entirely a random event and a decision is made during a period from initiation of DSBs to formation of dHJs (Hunter & Kleckner, 2001). In mice, it is reported that less than 10% of DSBs are repaired via DSBR (Cole et al., 2012). The DSBs are induced by an evolutionarily conserved protein, SPO11 transesterase, a DNA topoisomerase, during the leptotene stage (Fig. 2 & 3) (Keeney et al, 1997; Keeney, 2007). Facilitation of DSBs on unsynapsed chromosomes is critical for synapse completion, which is aided by localization of HORMA-domain protein 1 (HORMAD1) onto unsynapsed regions. CCDC36 (IHO1) is

directly associated with HORMAD1, which further recruits meiotic-specific transcription factor MEI4 and REC114 (Fig. 3). The complex of these proteins is proposed to promote DSB formation (Stanzione et al., 2016). After resection, 3' single-stranded ends enable strand exchange between homologs, referred to as single-end invasions (SEIs) (Hunter & Kleckner, 2001). During SEIs, ubiquitously expressed RAD51 and meiosis-specific DMC1 are loaded onto 3' tails to help search for intact homologous pairs of chromosomes (Fig. 2 & 3). Once homologous chromosomes are found, 3' single-stranded ends invade into homologous duplexes promoted by RAD51 and DMC1 to form D-loop structures (Sansam et al., 2015). In mammals, approximately 10-25% of DSBs are strictly controlled to produce crossovers (Reynolds et al., 2013). Recombination sites are subject to give rise to at least one crossover per homologous chromosome, defined as crossover assurance or obligatory crossover. In addition, multiple crossovers are not allowed to form close on one chromosome, referred as crossover interference (Hunter, 2015).

The majority of crossovers are generated by the interference-dependent (Class I) pathway (Holloway et al., 2008). Class I crossover formation is achieved by recruitment of a complex of recombination factors, including MutS_γ (MSH4-MSH5), RNF212, MutL_γ (MLH1/3), CDK2 and HEI10 (Fig. 3). MutS_γ, consisting of the MutS homolog 4-MutS homolog 5 (MSH4-MSH5), binds discretely at various recombination sites along homologous chromosome at the pachytene stage (Kneitz et al., 2000). Meanwhile,

RNF212, a central meiotic pro-crossover factor, selectively localizes onto MSH4-MSH5 sites to stabilize D-loops and form dHJs. RNF212-dependent SUMO modification further prevents the MSH4-MSH5-RNF212 complex from dissociation (Reynolds et al., 2013). Approximately half of MSH4-MSH5 marked sites progress into crossover sites, with the other half, without the stabilization of RNF212, dissolve and form non-crossovers (Santucci-darmanin et al., 2000). CDK2 and HEI10 (a cyclin E3 ubiquitin ligase), crossover-associated factor, associate with MSH4-MSH5–RNF212 marked foci to assist binding of MLH1/3, which is proposed to mark interfering crossover sites (Anderson et al., 1999; Lipkin et al., 2002; Ward et al., 2007).

A small subset of crossovers, approximately 5-10%, are formed by the alternative MUS81-EME1 pathway (Class II) (Holloway et al., 2011). The detailed mechanisms of this pathway have not yet been fully elucidated. But it is known that dimeric endonucleases MUS81 and EME1 function in rejoining DNA crosslinks and converting stalled DNA replication forks into DSBs (Hanada et al., 2006; Svendsen et al., 2009). At downstream steps of DNA damage repair, MUS81 and EME1 function as components of the Holiday junction resolvase, responsible for resolving X-shaped joint molecules to establish chiasmata (Boddy et al., 2001).

As SCs disassemble at later stages of meiosis prophase I, chiasmata formed by either Class I or Class II crossover pathways are resolved to allow for separation of homologous pairs at anaphase I (Hunter, 2015).

Polo-like kinases: function and mechanism

The discovery of polo-like kinases (PLK) originated from genetic screens of *Drosophila* designated to select maternal defects. They showed that homozygous mutant alleles of *Polo* in *Drosophila* give rise to abnormal meiotic division by forming multipolar spindles during spermatogenesis (Sunkel and Glover, 1988). A homolog of Polo was discovered in *Saccharomyces cerevisiae* (budding yeast), Cdc5, and was shown to be essential for cell division (Hartwell et al., 1973). However, in mammalian systems, there are five polo-like kinases, PLK1-PLK5, that are conserved in structure but varied in function (Fig. 4A) (de Cárcer, G. et al., 2011a). Polo-like kinases have a N-terminal serine/threonine kinase domain (KD) (except PLK5), and one or two C-terminal polo-box domains (PBD) (de Cárcer, G. et al., 2011). With respect to function, PLK1 coordinates processes during the cell cycle, such as DNA replication, mitotic entry, chromosome segregation and cytokinesis (Wu and Liu, 2008; Seki et al., 2008; Kang et al., 2006; Burkard et al., 2007). PLK2 and PLK3 have been shown to function during genotoxic stress responses (Matthew and El-Deiry, 2007; Bahassi et al., 2002). PLK4 is a key regulator of centriole duplication, and disruption of PLK4 levels leads to severe suppression of cell cycle progression (Habedanck et al., 2005). PLK5 accumulates specifically in brain and functions in neuron differentiation (de Cárcer, G. et al., 2011b).

The KD and PBD domains of PLK cooperate with one another to respond and transmit cellular signals to target proteins (Archambault et al., 2015). PBD is deprived of any

catalytic activity, but temporally and spatially regulates PLK subcellular localization (Lee et al., 1998). Proteomic screens discovered that PBD has a phosphoserine or phosphothreonine peptide binding motif (Elia et al., 2003). Such phosphopeptide binding domains are generated either via nonself-priming, usually by CDK1 or other kinases, or via PLK self-priming (Park et al., 2010). In addition, activation of the KD is regulated by phosphorylation events at the T-loop residue T210 or the hinge residue S137 sites via Aurora kinases (Fig. 4B) (Archambault and Carmena, 2012). The binding of the PBD to substrates enables the KD to phosphorylate its target. Although interactions between the two domains of polo-like kinases regulates their activities, phosphorylation of target proteins can be performed without binding to the PBD (Archambault et al., 2015).

Cdc5 and Polo-like kinase 1

Within the polo-like kinase family, PLK1 represents the most remarkable regulator of cell division. Functions of PLK1 on centrosomes and promotion of mitotic entry, on kinetochores and regulation of the spindle assembly checkpoint, and on cytokinesis have been characterized in many previous studies (Petronczki et al., 2008). However not much is known about its function during homologous recombination and the metaphase transition (G2/M1) during meiosis. Since the function of PLK1 resembles its homolog Cdc5 in budding yeast, we tried to bridge the findings in yeast to the mammalian system (Archambault et al., 2015). Work on Cdc5 has provided insights into the molecular mechanisms of polo-like kinases on meiotic recombination and during the G2/M1

transition. Meiotic depletion of Cdc5 caused defects in chiasmata formation (Clyne et al., 2003). Meiosis-specific transcription factor Ndt80 is a master regulator of many genes required for meiotic pachytene stage exit, including Cdc5 and cyclin-dependent kinase (CDK). Induced expression of Cdc5 in *ndt80*Δ mutated strains promoted joint molecule resolution at crossovers and SC disassembly (Sourirajan and Lichten, 2008). Both studies confirmed requirements for Cdc5 for pachytene exit during meiosis. Joint molecule resolution is carried out by a heterodimeric MUS81-EME1/MMS4 endonuclease (EME1 in mammals, MMS4 in *Saccharomyces Cerevisiae*). Resolvase activity is regulated by Cdc5-dependent phosphorylation (Gallo-Fernández et al., 2012). In mammalian systems, PLK1 has been elucidated to interact directly with another endonuclease factor, BTBD12 (SLX4 in budding yeast) and then interacts with MUS81-EME1 (Wyatt et al., 2013).

During the G2/M1 transition, BI 2536 was used as a selective inhibitor of PLK1 to prevent central elements from dissociation (Steggmaier et al., 2007). PLK inhibitor (BI 2536) treated mouse spermatocytes revealed that phosphorylation of central region proteins, including SYCP1, TEX12 and SYCE1 by PLK1 is required for SCs disassembly and the metaphase transition (Jordan et al., 2012).

In human somatic cells, cell culture-based studies have demonstrated that phosphorylation on S14 of RAD51 by PLK1 facilitates subsequent phosphorylation on T13 by CK2. The pT13/pS14 diphosphorylated RAD51 triggers recruitment to DNA damage sites (Yata et al., 2012). However, the interaction between PLK1 and DMC1, a

meiosis-specific version of RAD51, remains unknown. Based on these studies, it is of great interest to further characterize PLK1 functions during meiotic recombination in mammals.

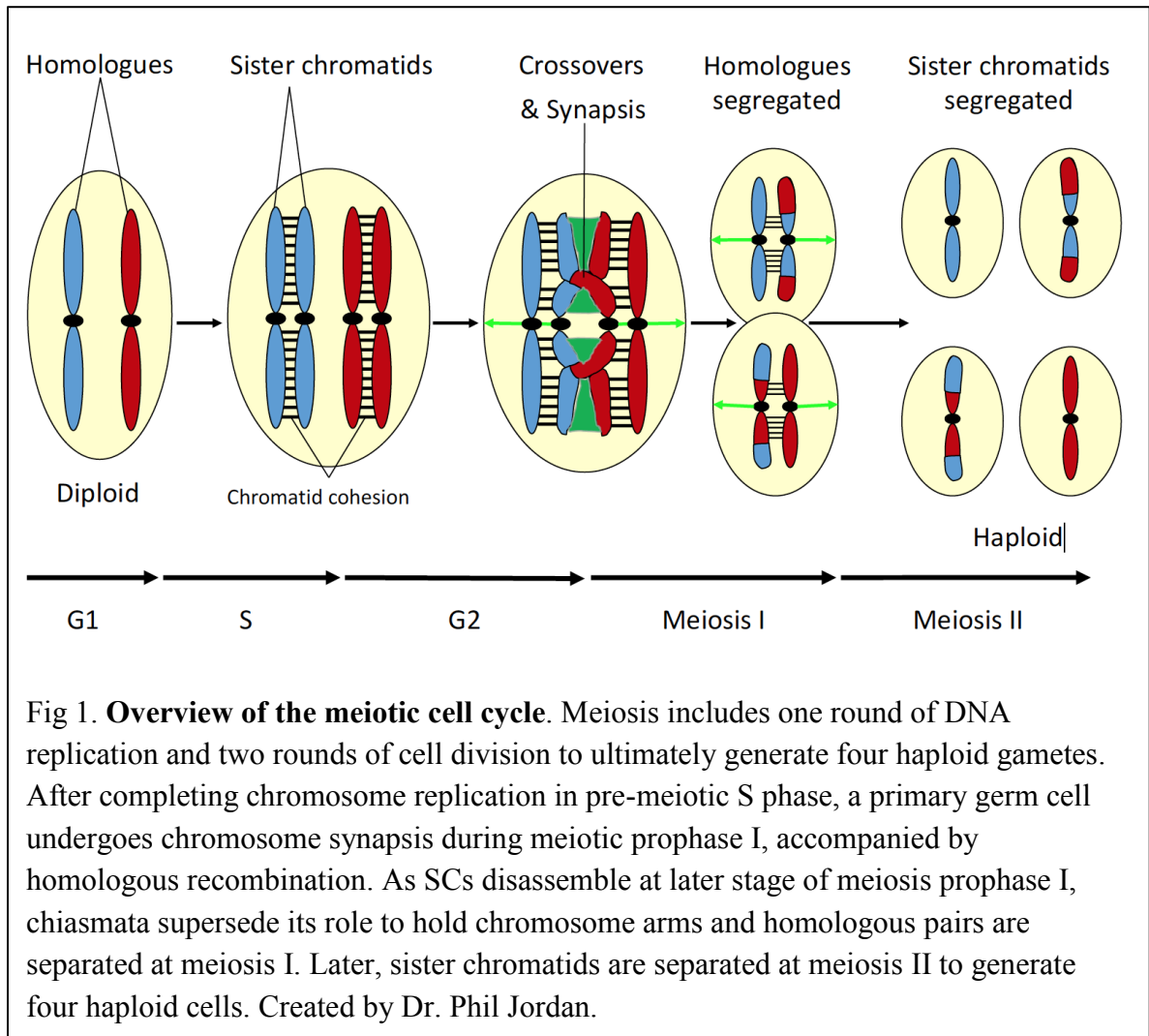


Fig 1. Overview of the meiotic cell cycle. Meiosis includes one round of DNA replication and two rounds of cell division to ultimately generate four haploid gametes. After completing chromosome replication in pre-meiotic S phase, a primary germ cell undergoes chromosome synapsis during meiotic prophase I, accompanied by homologous recombination. As SCs disassemble at later stage of meiosis prophase I, chiasmata supersede its role to hold chromosome arms and homologous pairs are separated at meiosis I. Later, sister chromatids are separated at meiosis II to generate four haploid cells. Created by Dr. Phil Jordan.

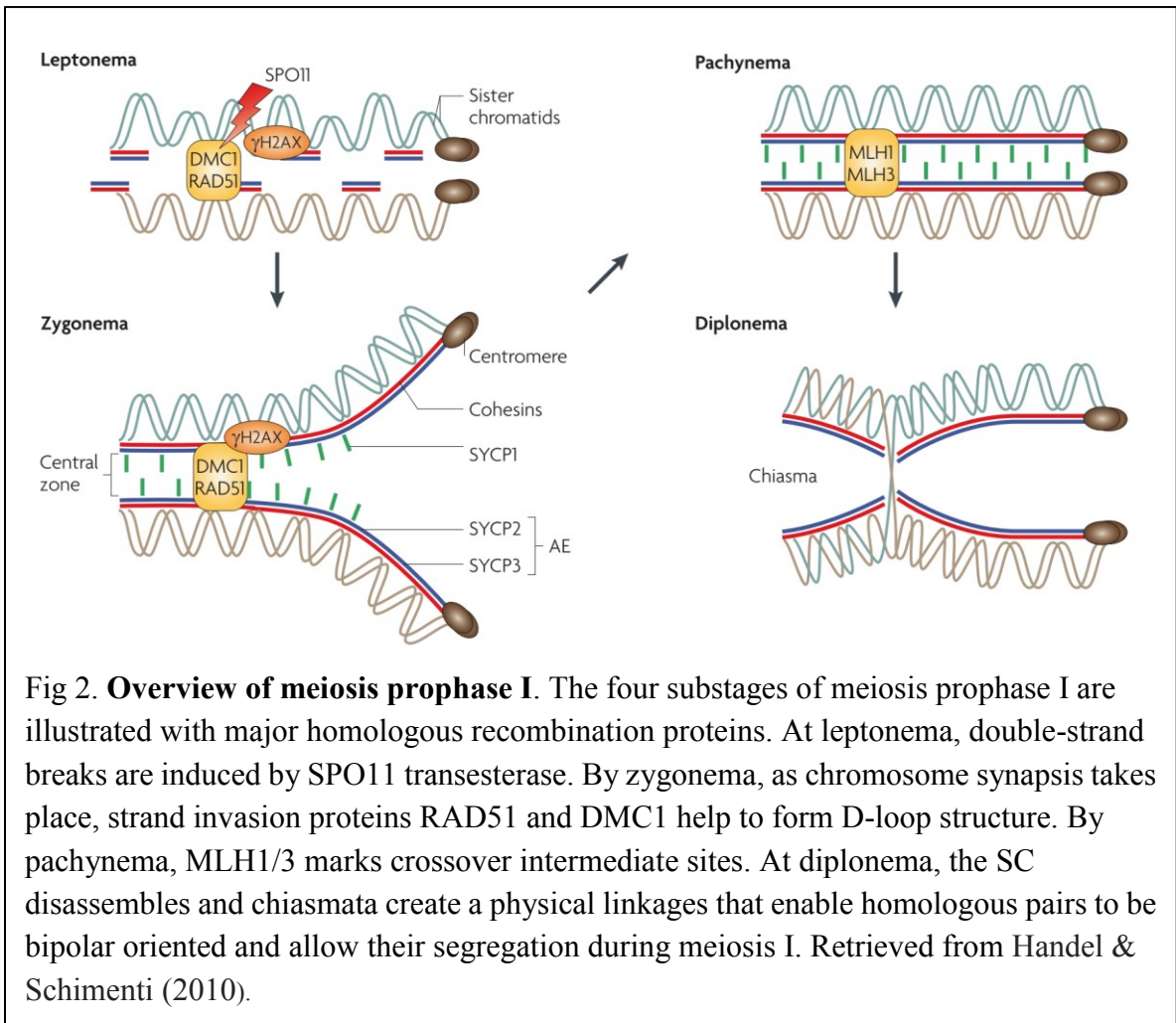


Fig 2. Overview of meiosis prophase I. The four substages of meiosis prophase I are illustrated with major homologous recombination proteins. At leptonema, double-strand breaks are induced by SPO11 transesterase. By zygonema, as chromosome synapsis takes place, strand invasion proteins RAD51 and DMC1 help to form D-loop structure. By pachynema, MLH1/3 marks crossover intermediate sites. At diplonema, the SC disassembles and chiasmata create a physical linkages that enable homologous pairs to be bipolar oriented and allow their segregation during meiosis I. Retrieved from Handel & Schimenti (2010).

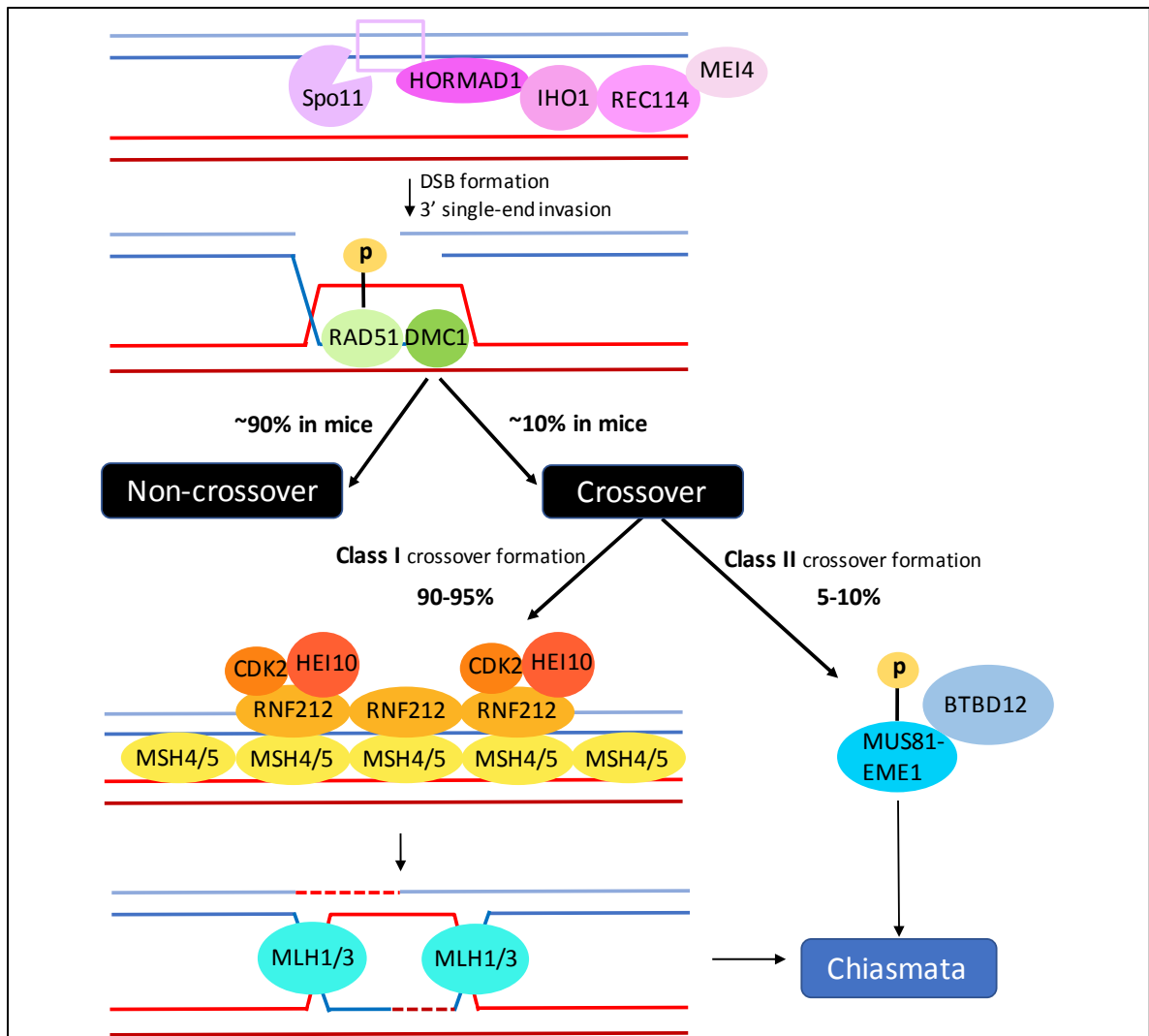
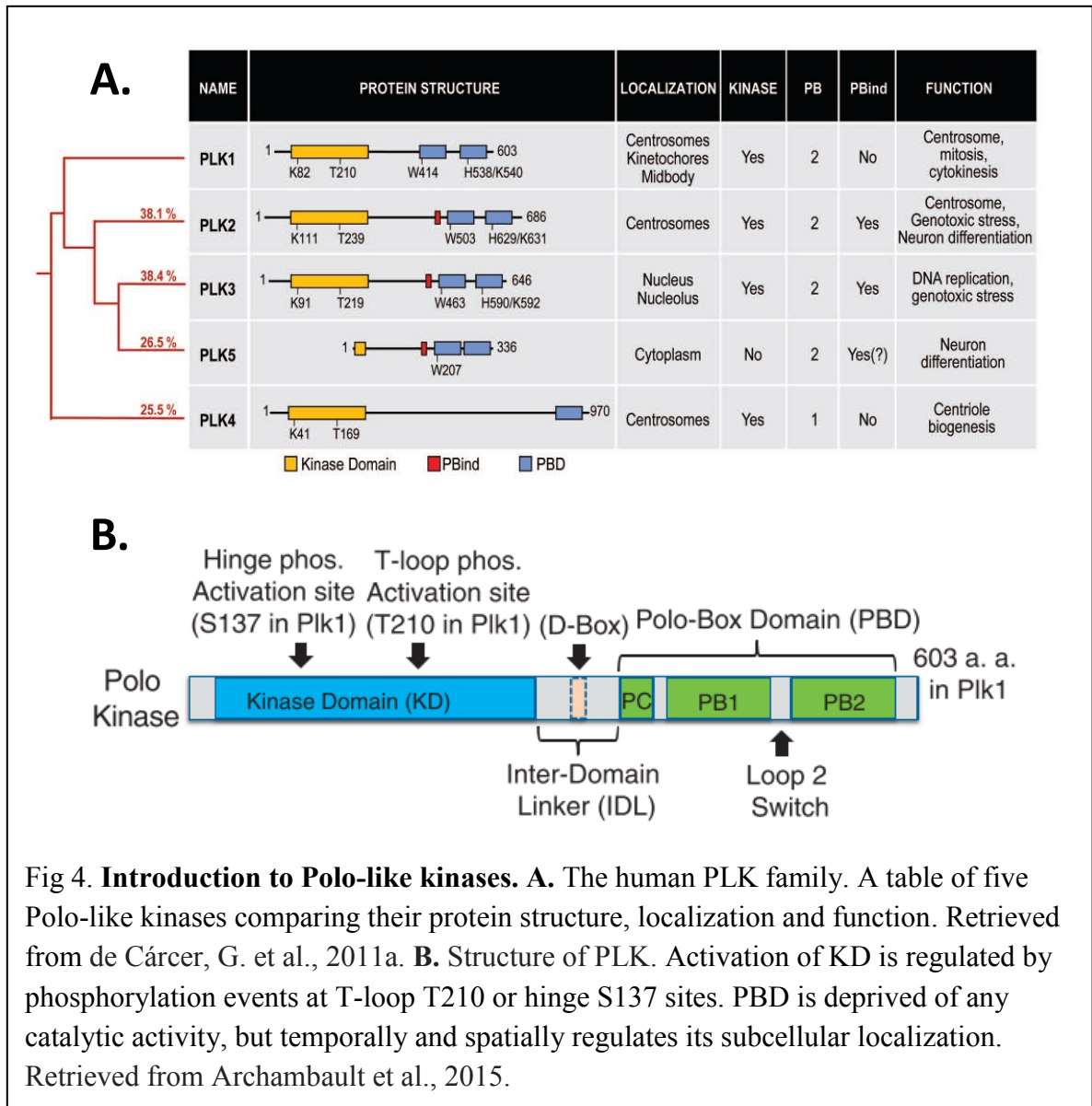


Fig 3. Overview of homologous recombination. Schematic diagram displays major homologous recombination proteins, emphasized on crossover pathway and key transition. During meiotic prophase, homologous recombination is programmed to ensure physical association between homologous chromosomes, which ensures accurate chromosome segregation during meiosis. Recombination occurs within the context of a protein scaffold known as the synaptonemal complex, which bridges homologs. Homologous recombination initiates with SPO11-induced double-strand breaks, promoted by HORMAD1 and IHO1. After resection, ubiquitously expressed RAD51 and meiosis-specific DMC1 are loaded onto 3' tails to invade into homologous duplex, forming a D-loop structure. Crossovers are generated by two pathways: Class I and Class II. The majority of crossovers are formed by MSH4/5 and MLH1/3 Class I pathway. A subset of crossovers are made by MUS81-EME1 Class II pathway.



MATERIALS AND METHODS

Ethic statement

All mice were bred at Johns Hopkins University (JHU, Baltimore, MD) under standard conditions in accordance with the National Institutes of Health (NIH) and US Department of Agriculture criteria. Protocols for their care and use were approved by the Institutional Animal Care and Use Committees (IACUC) of JHU.

Mice

Mice $Plk1^{tm1c(EUCOMM)Hmgu}$ (designated $Plk1^{+/FloX}$), harboring $Plk1$ with a floxed exon 3 were used as control in this study. Heterozygous mice $Plk1^{tm1d(EUCOMM)Hmgu}$ (designated $Plk1^{+/Del}$), harboring $Plk1$ with a deleted exon 3 were bred to mice harboring the $Spo11$ -Cre transgene [C57BL/6-Tg(Spo11-cre)1Rsw/J], which gave rise to progeny heterozygous for the $Plk1^{del}$ allele and hemizygous for the $Spo11$ -Cre transgene ($Plk1^{+/Del}$, $Spo11$ -Cre tg/0). Male $Plk1^{+/Del}$, $Spo11$ -Cre tg/0 mice were bred to homozygous female $Plk1^{FloX/FloX}$ mice to derive $Plk1$ cKO (designated $Plk1^{FloX/Del, Spo11-Cre}$). The $Plk1^{+/FloX, Spo11-Cre}$ and $Plk1^{FloX/Del}$ genotype were used as additional controls.

PCR genotyping

Genotyping of mice was done by polymerase chain reaction (PCR). Mice tail tip was harvested and digested by 50 mM NaOH at 95 °C for 15 mins. The mixture was added with 1M Tris-HCl pH 8.0 and used as DNA template for PCR. Each PCR reaction consisted of molecular grade water, AccuStart II PCR SuperMix, oligo primers, and DNA template (see

Table 1) PCR was set by following condition: 90°C for 2 min, and 30 cycles of 90°C for 20 s; 58°C for 30s; and 72°C for 1 min. PCR products was analyzed by 2% agarose gel.

Primers used in this study were shown in Table 2.

Table 1. PCR set up for one sample

Stock	1x
H ₂ O	4.75
AccuStart II PCR SuperMix	6.25
Oligo primers	0.25
DNA template	1

Table 2. Primers used in this study

Gene	Forward primers (5'-.....-3') Reverse primers (5'-.....-3')	Expected band size
<i>Spo11-Cre</i>	CCATCTGCCACCAGCCAG TCGCCATCTTCCAGCAGG	Spo11-Cre=281 bp
<i>Cpxm1</i>	ACTGGGATCTTCGAACTCTTTGGAC GATGTTGGGGCACTGCTCATTACC	WT= 420 bp
<i>Plk1_Del</i>	AGTATGGCAGGCAGCATCTC ATGCTCCATGGAAAGTCAGG	Flox= 1174 bp WT= 1012 bp Del= 341 bp
<i>Plk1_Flox</i>	CTAGCACTGAGCCAGACCCTCAGC GGATAGCAGAATTAGATGCACTGG	WT= 221 bp Flox= 355 bp

Histology and TUNEL assay

Adult testis tissues were fixed in bouins fixative. Tissues were embedded in paraffin and serial sections 5 microns thick were placed onto slides and stained with hematoxylin and eosin (H&E). For TdT-mediated dUTP nick end labelling (TUNEL) assay, tissues were deparafnized by sequential wash in xylene, 100% ethanol, 95% ethanol, 85% ethanol, 70% ethanol, 50% ethanol, 0.85% NaCl, and 1X PBS. TUNEL positive cells were

detected using the in situ BrdU-Red DNA fragmentation (TUNEL) assay kit (Abcam) and stained with 4', 6-diamidino-2 phenylindole (DAPI).

Spermatocyte chromosome microspreads

Isolation of germ cells from testis was performed using two methods:

1) One technique was previously described (Bellve 1993; La Salle et al. 2009). Germ cells were isolated from mice from 15 to 19 days post-partum (dpp), enriched with meiosis prophase I spermatocytes. Mice were sacrificed by cervical dislocation, both testes were placed in 1X phosphate buffered saline (PBS) and tunica albicans were removed. Testis tubules were minced using flathead forceps in Krebs-Ringer bicarbonate solution (KRB) (see Table 3). Cell suspension was filtered using 0.8 μ m Nitex mesh. After centrifuge at 9K rpm for 5 min, supernatant was discarded and cells were resuspended with 0.1M sucrose solution (see Table 4). Cells were placed on slides incubated with 1% Paraformaldehyde (PFA) solution (see Table 5). Slides were placed in a dark moist chamber overnight. Slides were washed first in 0.2% photoflo in 1X PBS and then in Antibody Dilution Buffer (ADB) (see Table 6).

2) The other technique was also previously described (Watanabe & Nurse, 1999). Germ cells were isolated from mice from 15 to 19 days post-partum (dpp). Mice were sacrificed by cervical dislocation, both testes were harvested and tunica albicans were removed. Testis tubules were minced using flathead forceps in Krebs-Ringer bicarbonate solution (KRB). Cell suspension was filtered using 0.8 μ m Nitex mesh. After centrifuge at

3k rpm for 6min, supernatant was discarded and cells were resuspended in hypotonic buffer (see Table 7). After another centrifuge at 3k rpm for 6min, supernatant was discarded and cells were resuspended with 0.1mM sucrose solution. Cells were placed on slides incubated with 1% PFA solution. Slides were placed in a dark moist chamber for an hour, dried for another hour, and washed overnight in 0.4% photoflo in 1X PBS. Slides were left to air dry, and washed in Antibody Dilution Buffer (ADB).

Table 3. Krebs-Ringer bicarbonate solution (KRB)

Stock solution	2000 mL	Final Concentration
9% NaCl	156 mL	120 mM
1.15% KCl	62.4 mL	4.8 mM
6.5% NaHCO ₃	65.2 mL	25.2 mM
2.1% KH ₂ PO ₄	15.6 mL	1.2 mM
3.8% MgSO ₄ 7H ₂ O	15.6 mL	1.2 mM
1.2% CaCl	23.4 mL	1.3 mM
100X penicillin-Streptomycin-glutamine	20 mL	1X
100X MEM non-essential amino acids	40 mL	1X
100X MEM essential amino acids	20 mL	1X
Dextrose	4 g	11.1 mM
DDH ₂ O to	2000mL	

Table 4. 0.1M sucrose solution, pH to ~8.0

Stock solution	5 mL	Final Concentration
0.5M Sucrose	1 mL	0.1M
MilliQH ₂ O	4 mL	N. A
50mM NaOH	100 µL	Bring pH to ~8.0
50X protease inhibitor	20 µL	0.2X

Table 5. 1% Paraformaldehyde (PFA), pH to ~8.0

Stock solution	10 mL	Final Concentration
16% PFA	625 µL	1%
MilliQH ₂ O	9.375 mL	N. A

50mM NaOH	120 μ L	Bring pH to ~8.0
50X protease inhibitor	40 μ L	0.2X
10% Triton X-100	10 μ L	0.01%

* 16% paraformaldehyde, EM grade, from Electron Microscopy Sciences, Cat.

Number: 15710

Table 6. Antibody Dilution Buffer (ADB)

Stock solution	500 mL	Final Concentration
10X PBS	50 mL	1X
BSA	15 g	3%
Horse serum	50 mL	10%
Triton X-100	250 μ L	0.05%
MilliQH ₂ O to	500 mL	

* Filtered with 0.2 μ m filter

Table 7. Hypotonic buffer

Stock solution	40 mL	Final Concentration
600mM Tris	2 mL	30mM
500mM Sucrose	4 mL	50mM
170mM Citric Acid	4 mL	17mM
500mM EDTA	400 μ L	5mM
50X protease inhibitor	160 μ L	

Immunofluorescence microscopy

Primary antibodies used and dilution factor are listed in Table 8. Secondary antibodies against human, rabbit, rat, mouse and guinea pig IgG and conjugated to Alexa 350, 488, 568 or 633 (Life Technologies) were used at 1:500 dilution. Spermatocyte chromatin spreads were mounted with Vectashield + DAPI medium (Vector Laboratories). Images were captured using a Zeiss Cell Observer Z1 linked to an ORCA-Flash 4.0 CMOS camera

(Hamamatsu) and analyzed with the Zeiss ZEN 2012 blue edition image software.

Photoshop (Adobe) was used to prepare figure images.

Table 8. Primary antibodies used in this study

Antibodies	Host	Source	Cat. Number	IF Dilution
CDK2	Mouse	Santa Cruz	sc-6248	1:50
CEN	Human	Antibodies Incorporated	15-235	1:50
DMC1	Mouse	Abcam	ab11054	1:100
IHO1	Guinea pig	Attila Toth's lab		1 : 500
MLH1	Mouse	Thermo	MA5-15431	1:100
RAD51	Mouse	Thermo	PA527195	1:50
SYCP3	Rabbit	Novus	NB300-231	1 : 1000
SYCP3	Rabbit	Abcam	ab15093	1 : 500

Statistical analysis

Statistical data was collected using Adobe Photoshop CC 2017 and Image J software.

Data was organized by Microsoft Excel. Statistical analysis was performed using

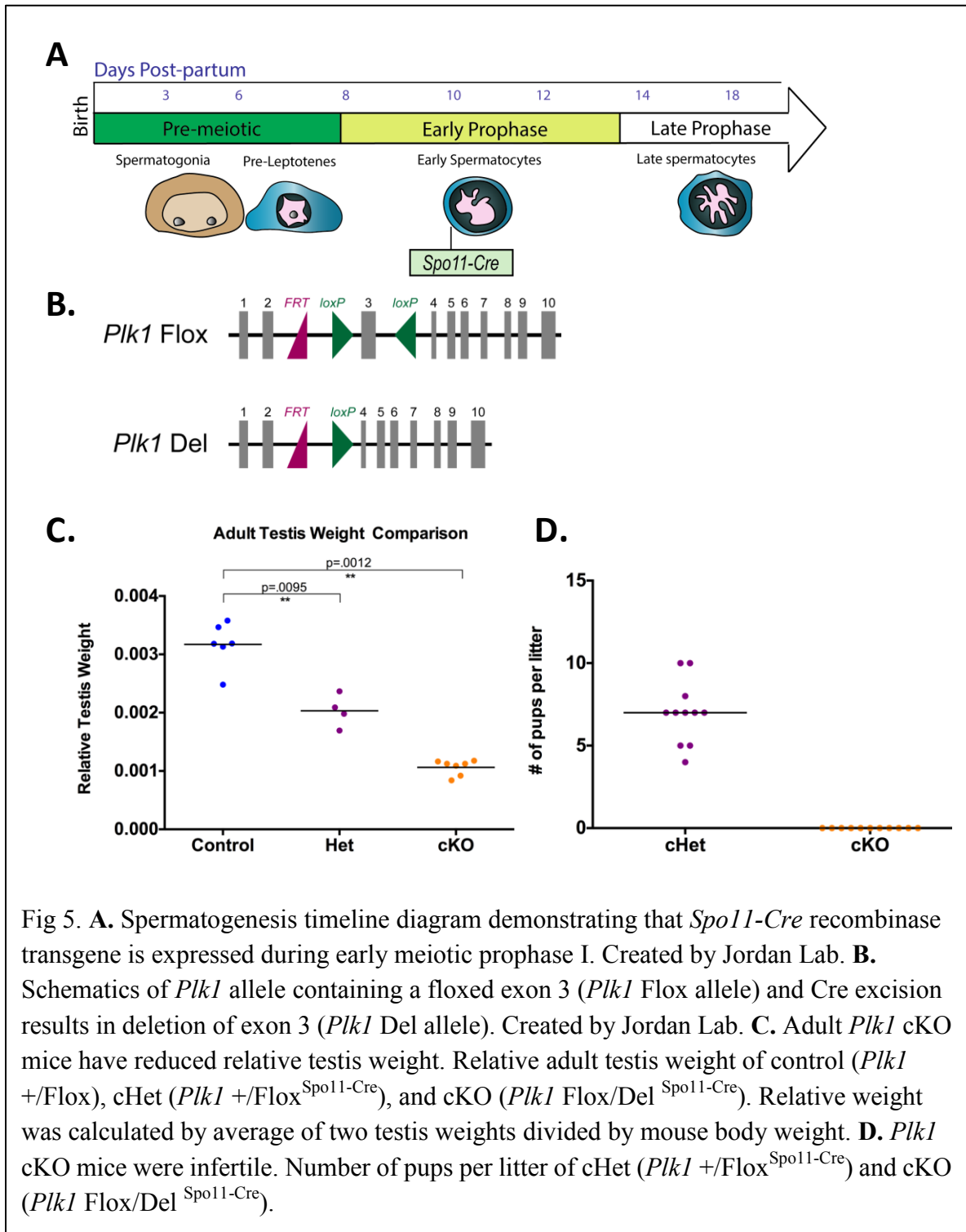
GraphPad Prism 6.

RESULTS

Conditional knockout of *Plk1* during spermatogenesis results in meiotic aberrancies and sterility

Mice that harbored a germ-cell-specific conditional knockout allele of *Plk1*, designated as Flox/Del^{Spo11-Cre} (cKO) were used to access the requirement of *Plk1* for DNA damage response during spermatogenesis (See Materials and Methods). Exon3 of *Plk1* was flanked by *loxP* sites and was deleted during early meiosis prophase I, driven by a hemizygous *Spo11-Cre* recombinase transgene. Spo11 transesterase, a DNA topoisomerase, is an inducer for DSBs at the leptotene stage (Fig. 4A&B) (Keeney et al, 1997; Keeney, 2007). Conditional knockout of *Plk1* was confirmed by gene analysis (See Materials and Methods). *Plk1* +/Flox (Control) mice, conditional heterozygous *Plk1* +/Flox^{Spo11-Cre} (cHet) mice, heterozygous *Plk1* Flox/Del (Het) mice and cKO mice had distinct phenotypes regarding testis weight and fertility. The average relative testis weight of adult Het mice was 36.0% smaller than their adult littermate controls. However, for adult cKO mice, the average relative testis weight was 64.6% smaller than their adult littermate controls (n=6 for control; n=4 for Het; n=7 for cKO) (Fig. 4C). Assessment of fertility showed that cKO mice had no offspring, as compared with cHet mice giving birth to an average of 7 pups per litter (n=11 for Het and cKO) (Fig. 4D). According to hematoxylin and eosin staining performed on adult mouse testis, at various stages of spermatogenesis, control mice and cHet mice showed indistinguishable generations of

germ cells within each section of seminiferous tubule. However, histological cross-sections of cKO mice lacked mature spermatids and contained enlarged primary spermatocytes (Fig. 6A). Based on statistical analysis on histological cross-sections, cKO mice had seminiferous tubules with reduced diameters and decreased numbers of cells per tubule cross area as compared to control mice ($p < .0001$) (Fig. 6B). TUNEL stained cross-sections displayed an increased number of apoptotic cells in *Plkl* cKO testes (Fig. 5A). Quantification of tubule cross-sections with TUNEL positive staining showed that 36.6% of tubules with TUNEL positive staining in cKO mice had while control mice had 0.87% and cHet had 16.23% (Fig. 5B).



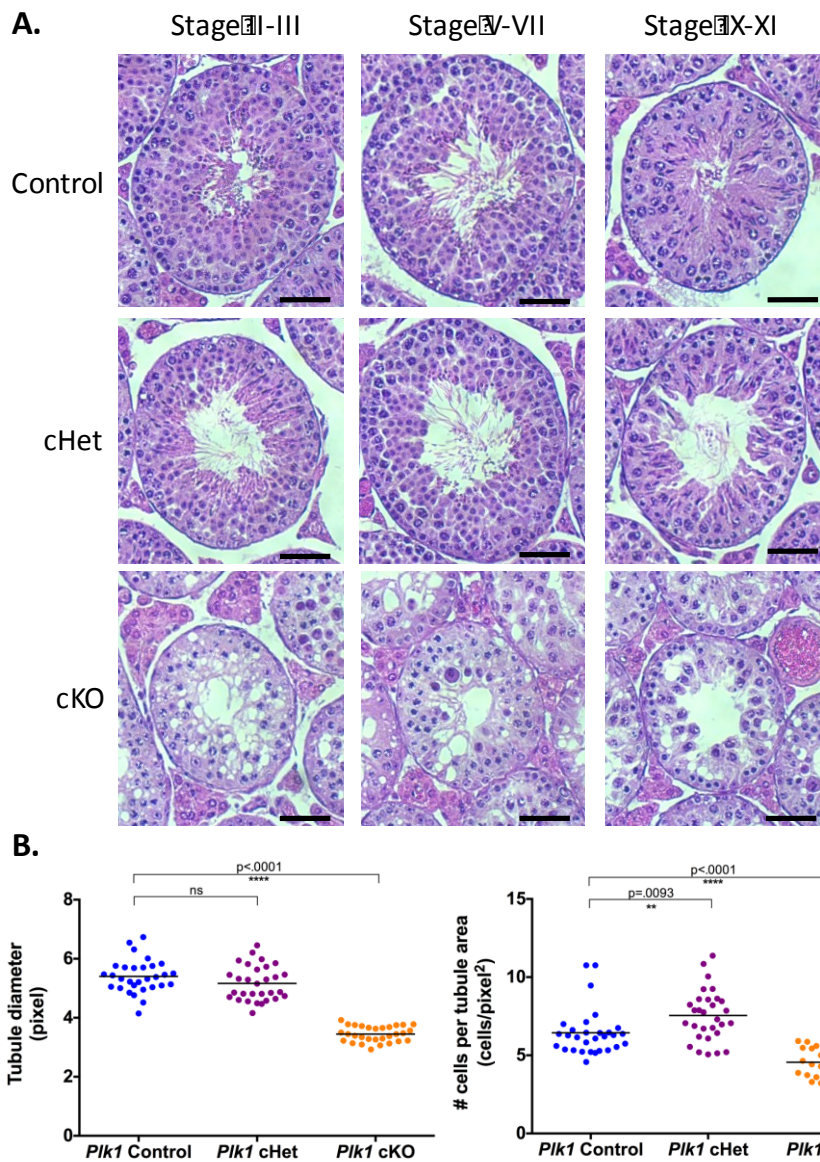


Fig 6. **A.** Hematoxylin and eosin stained seminiferous tubule cross-sections of 96 dpp mouse testis at various stages of spermatogenesis. Bar length: 50 μ m (x20 magnification). **B.** *Plk1* cKO mice have seminiferous tubules with reduced diameters and fewer cells per tubule cross area. Tubule diameter of control (*Plk1* +/Flox), cHet (*Plk1* +/Flox^{Spo11-Cre}), and cKO (*Plk1* Flox/Del^{Spo11-Cre}). Diameter was measured in pixel by imageJ. Number of tubules analyzed: control, n= 30; cHet, n=30; cKO, n=30. P values were calculated by two-tailed Mann-Whitney test. Number of cells per tubule area of control (*Plk1* +/Flox), cHet (*Plk1* +/Flox^{Spo11-Cre}), and cKO (*Plk1* Flox/Del^{Spo11-Cre}). Number of cells was counted by imageJ. Tubule area was measured in pixel² by imageJ. Number of tubules analyzed: control, n= 30; cHet, n=30; cKO, n=30. P values were calculated by two-tailed Mann-Whitney test.

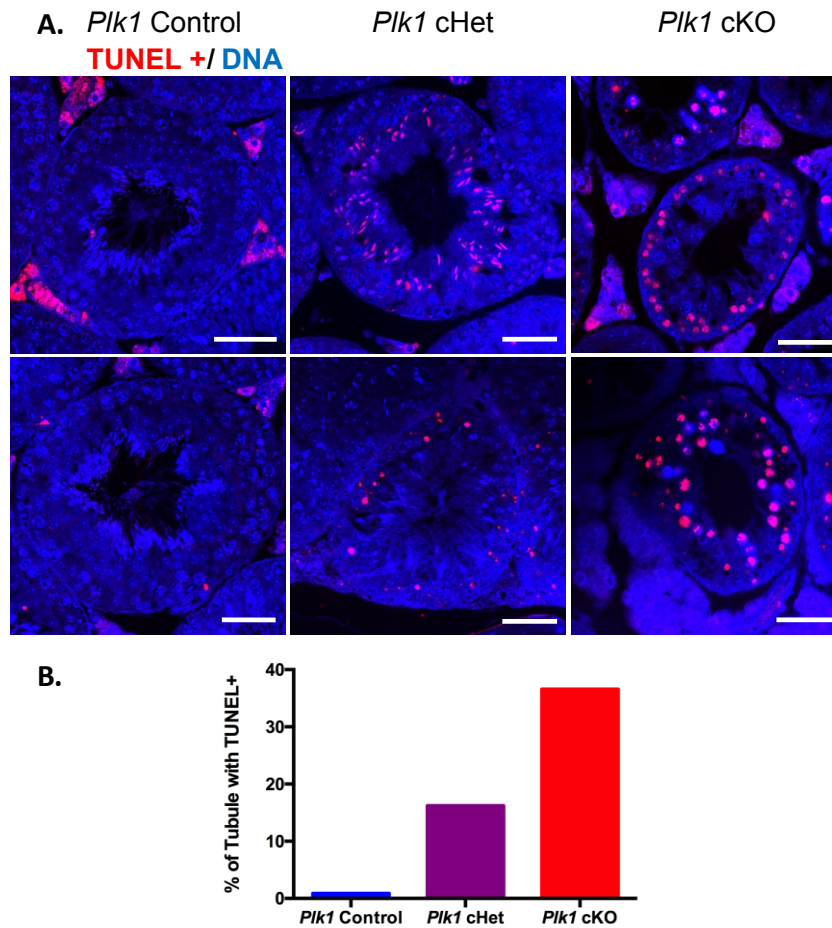
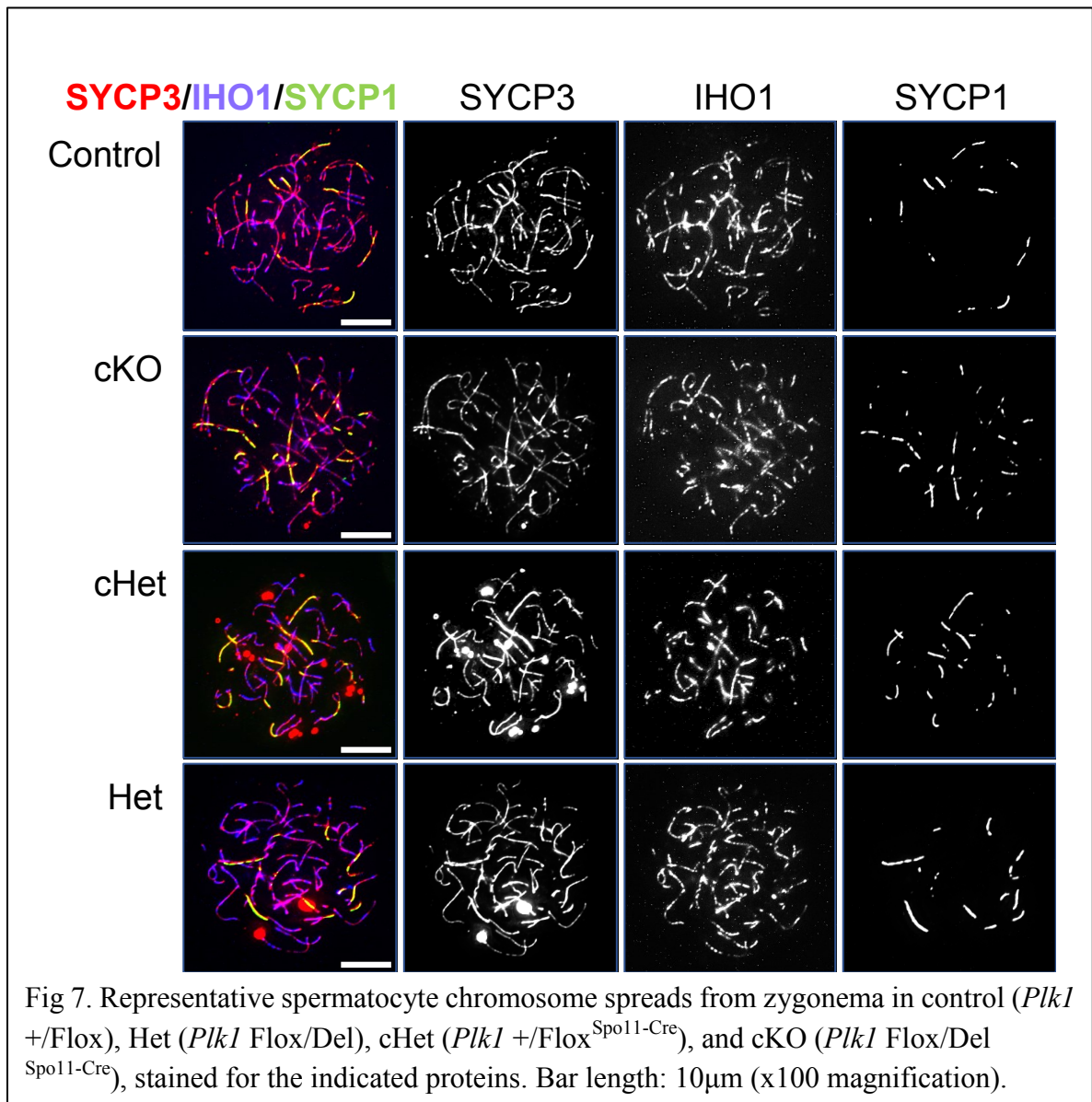


Fig 5. **A.** TUNEL stained cross sections of 96 days post-partum (dpp) mouse testis of control (*Plk1* +/Flox), cHet (*Plk1* +/Flox^{Spoll1-Cre}), and cKO (*Plk1* Flox/Del^{Spoll1-Cre}). Bar length: 50 μ m (x40 magnification). **B.** *Plk1* cKO cross-section of seminiferous tubule has increased number of apoptotic cells. Quantification of % of tubule with TUNEL positive staining. Number of tubules analyzed: control, n= 231; cHet, n=191; cKO, n=194.

***Plk1* cKO does not impact IHO1, a protein required for DSB formation**

To understand the morphological abnormality in testis cross-sections, we first checked whether defects showed up at the beginning of homologous recombination. We assessed a protein required for DSB formation, CCDC36 (IHO1). It is known that IHO1 is directly associated with HORMAD1, marking unsynapsed regions of chromosomes (Stanzione et al., 2016). SYCP1 is a transverse filament that makes up the central region of the SC, marking synapsed regions of chromosomes (Fraune et al., 2012). Merging individual channels of IHO1 and SYCP1 showed similar alignments with SYCP3 in all genotypes of spermatocytes, indicating that there's no difference in IHO1 localization (Fig. 7). Since only IHO1 is assessed at this point, we assume that PLK1 may not have a role on DSB formation.



***Plk1* cKO spermatocytes have reduced early recombination intermediates**

To determine whether DNA damage repair was compromised in early meiosis, we assessed an early homologous recombination intermediate. RAD51 and DMC1 are single-strand invasion proteins, which help search for intact homologous pairs of chromosomes and promote formation of D-loop structures (Sansam et al., 2015). It is known that recruitment of RAD51 to single-strand sites is facilitated by PLK1-dependent phosphorylation (Yata et al., 2012). In our *Plk1* cKO mice, we observed a reduction in RAD51 foci number (Fig. 8A). Mean RAD51 foci number at late zygonema was 93.9 for control spermatocytes, whereas 126.3 for cKO spermatocytes (n=12 for control; n=9 for cKO) (Fig. 8B). Mean RAD51 foci number for Het and cHet spermatocytes were 129.3 and 132.7 respectively (n=12 for Het; n=21 for cHet). By pachynema, mean RAD51 foci numbers, excluding the sex body, evenly reduced to 28.5, 41.5, 42.3, and 39 for control, Het, cHet, and cKO spermatocytes, respectively (n=14 for control; n=15 for Het; n=14 for cHet; n=14 for cKO).

Since DMC1 is a meiosis-specific version of RAD51, we were interested in determining whether PLK1 is required for DMC1 localization and function. We used our cKO mice to assess the number of DMC1 foci at late zygonema and early pachynema (Fig. 9A). The average number of DMC1 foci was 133.2 at late zygonema for control spermatocytes (n=36). Remarkably, average DMC1 foci numbers from the other three genotypes (Het, cHet, cKO) were uniformly reduced by ~40% as compared with control

spermatocytes (Fig. 9B). Het, cHet, and cKO spermatocytes had average DMC1 foci numbers of 87.5, 86.4, and 85.1, respectively (n=20 for Het; n=38 for cHet; n=24 for cKO). At early pachytene stage, DMC1 starts to dissociate from chromosome arms. The mean DMC1 foci numbers, excluding the sex body, normalized to be equivalent to control, which was about 30 foci (Fig 9B). cKO spermatocytes had an average DMC1 foci number of 36.5, which was not significantly different from control spermatocytes with a mean number of 33.3 (n=15 for control; n=12 for cKO).

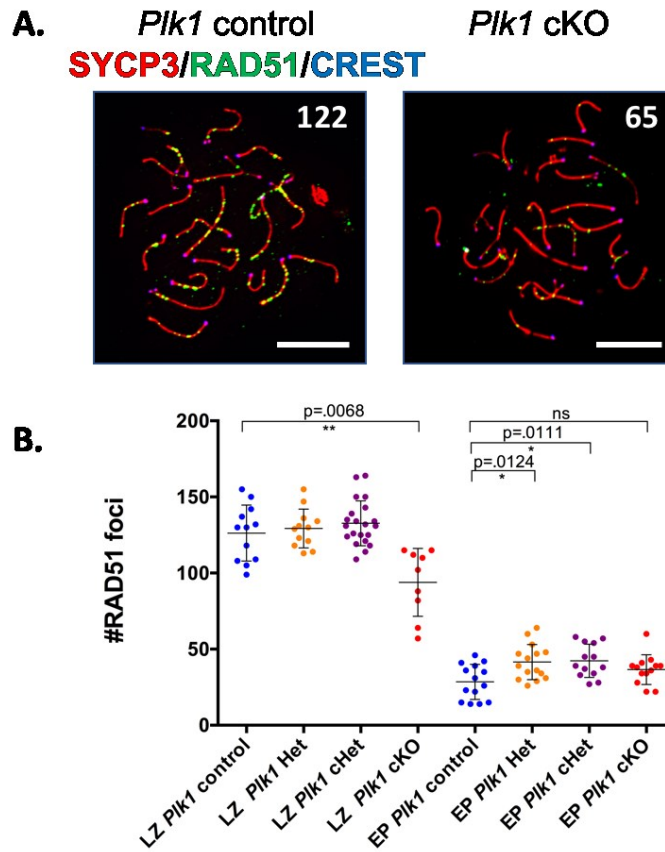
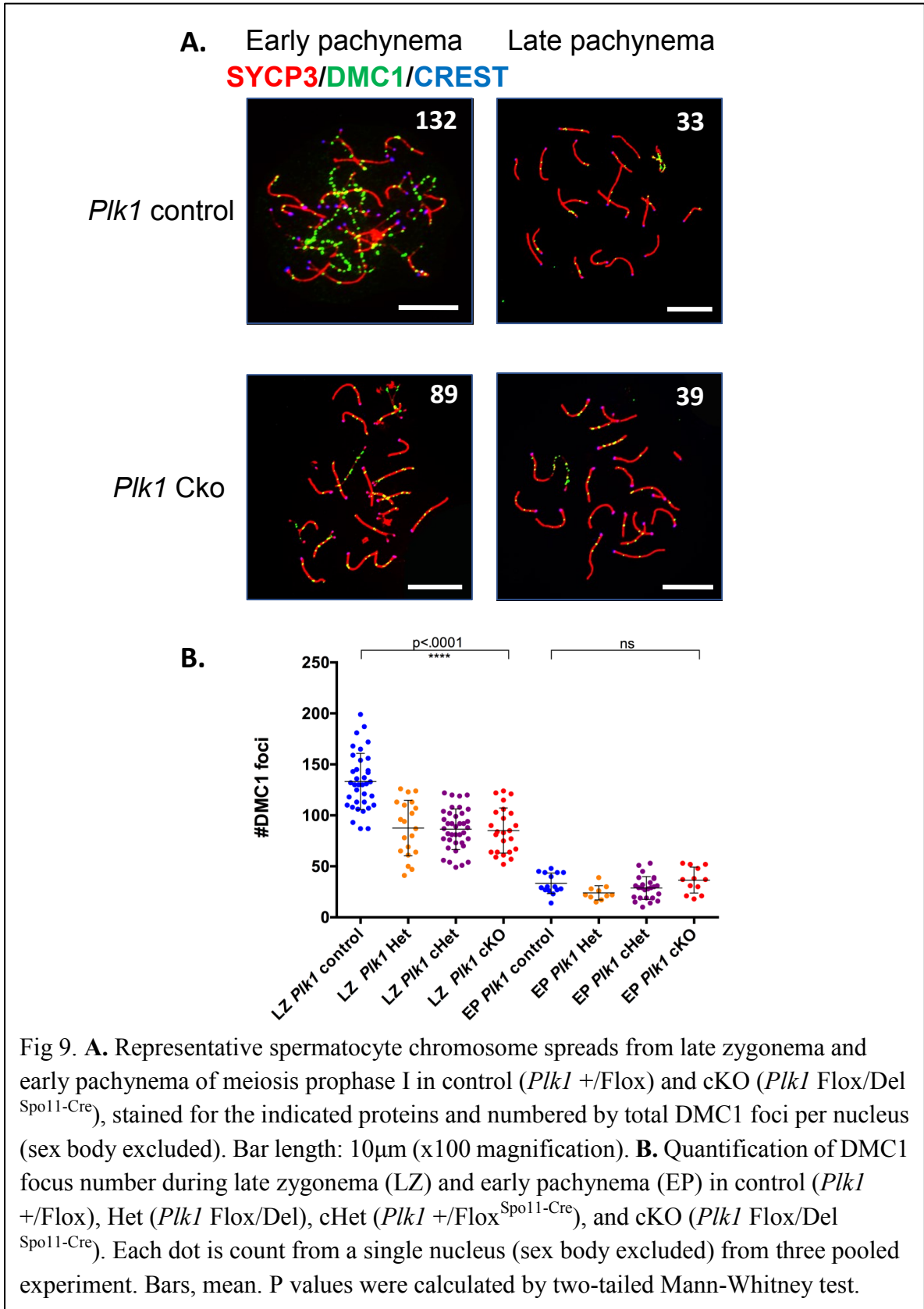


Fig 8. **A.** Representative spermatocyte chromosome spreads from late zygonema in control (*Plk1* +/Flox) and cKO (*Plk1* Flox/Del^{Spo11-Cre}), stained for the indicated proteins and numbered by total RAD51 foci per nucleus. Bar length: 10 μ m (x100 magnification). **B.** Quantification of RAD51 focus number during late zygonema (LZ) and early pachynema (EP) in control (*Plk1* +/Flox), Het (*Plk1* Flox/Del), cHet (*Plk1* +/Flox^{Spo11-Cre}), and cKO (*Plk1* Flox/Del^{Spo11-Cre}). Each dot is count from a single nucleus (sex body excluded) from one or two pooled experiment. Bars, mean. P values were calculated by two-tailed Mann-Whitney test.



***Plk1* cKO spermatocytes have increased numbers of MLH1 marked crossovers**

A small subset of crossovers is generated by the MUS81-EME1 Class II pathway (Holloway et al., 2011). In budding yeast, the function of the MUS81-EME1 endonuclease complex is positively regulated by PLK (Cdc5)-dependent phosphorylation (Gallo-Fernández et al., 2012). A previous study showed that in the absence of mammalian MUS81 or its interactive protein BTBD12, the normal flux towards Class II is lost. Instead, additional MLH1/3 foci are recruited to restore chiasmata counts (Holloway et al., 2011). We therefore hypothesized that if we disrupted PLK1 in the mouse testis, we would have a block towards the Class II MUS81-EME1 pathway, driving a shift towards the Class I MLH1/3 pathway and resulting in an increased number of MLH1/3 foci. We addressed this hypothesis by assessing the number of MLH1 in our *Plk1* cKO spermatocytes at mid-pachynema (Fig. 10A). The average number of MLH1 foci at mid-pachynema for control spermatocytes was 23.0 (n=59). Remarkably, cKO spermatocyte had an increased number of MLH1 foci with an average of 25.0 (n=66) at mid-pachynema, showing an 8.7% increase in number of MLH1 foci (Fig. 10B). Mean MLH1 foci numbers of Het and cHet spermatocytes are 23.6 and 23.3 respectively, matched with control spermatocytes (n=12 for Het; n=21 for cHet). Although crossover sites increased, inter-focus distance between MLH1 foci showed the same degree of crossover interference (Fig. 11).

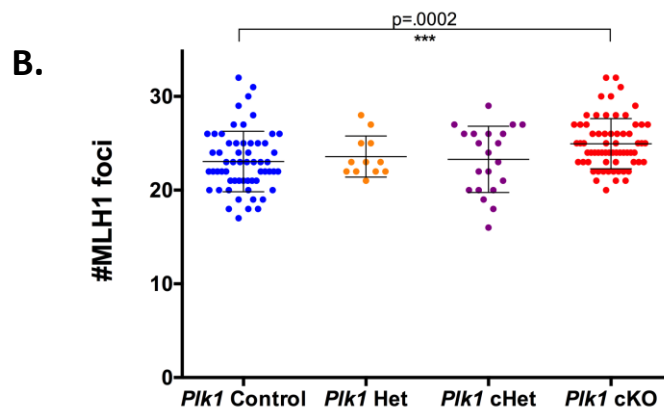
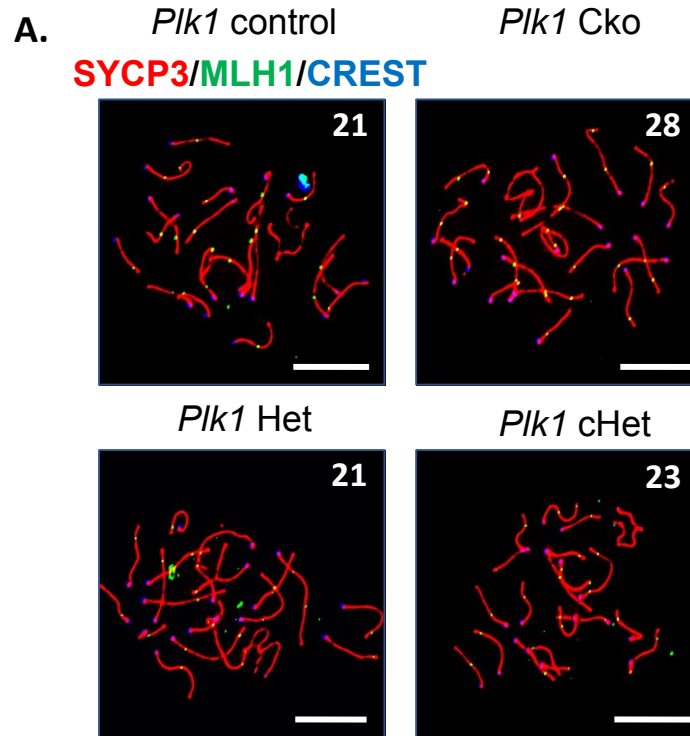


Fig 10. **A.** Representative spermatocyte chromosome spreads from mid-pachynema in control (*Plk1* +/Flox), Het (*Plk1* Flox/Del), cHet (*Plk1* +/Flox^{Spo11-Cre}), and cKO (*Plk1* Flox/Del^{Spo11-Cre}), stained for the indicated proteins and numbered by total MLH1 foci per nucleus. Bar length: 10 μ m (x100 magnification). **B.** Quantification of MLH1 focus number during mid-pachytene in control (*Plk1* +/Flox), Het (*Plk1* Flox/Del), cHet (*Plk1* +/Flox^{Spo11-Cre}), and cKO (*Plk1* Flox/Del^{Spo11-Cre}). Each dot is count from a single nucleus from four pooled experiment. Bars, mean. Number of spermatocyte analyzed: control, n=59; Het, n=12; cHet, n=21; cKO, n=66. (with the help of HIT as a staging indicator). P values were calculated by two-tailed Mann-Whitney test.

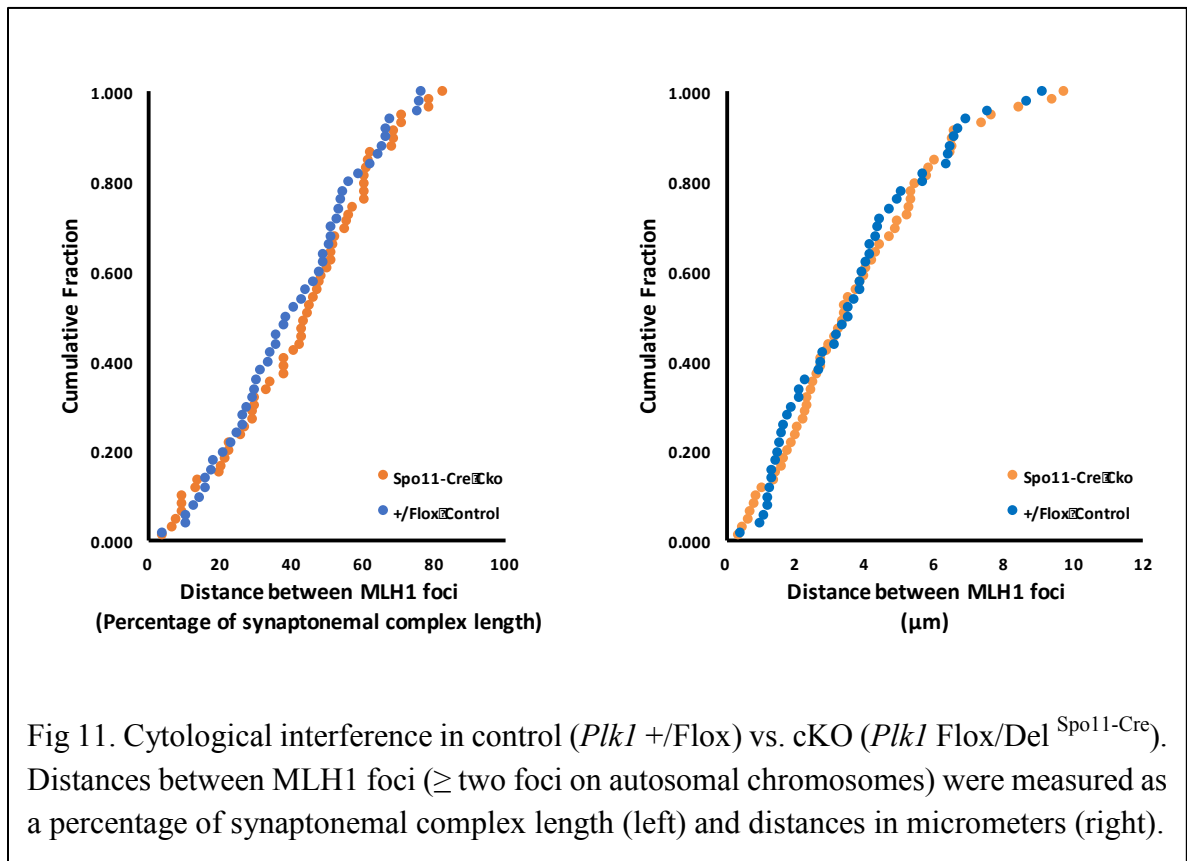


Fig 11. Cytological interference in control (*Plkl* +/Flox) vs. cKO (*Plkl* Flox/Del^{Spo11-Cre}). Distances between MLH1 foci (\geq two foci on autosomal chromosomes) were measured as a percentage of synaptonemal complex length (left) and distances in micrometers (right).

***Plk1* cKO spermatocytes have an increase in crossover-associated CDK2 foci**

To support that additional MLH1/3 Class I events take place when PLK1 levels are disturbed, we assessed a pro-crossover protein CDK2 for interference establishment (Fig. 12A). Control spermatocytes had an average number of 18.3 crossover (CO)-associated CDK2 foci at mid-pachynema, excluding the sex body (n=20). Interestingly, cKO spermatocytes showed an increased number of CO-associated CDK2 foci with an average of 22.04, excluding the sex body, showing a 20.4% increase in number of CO-associated foci as compared to control spermatocytes. Meanwhile, cHet and Het spermatocytes showed matching phenotype as control spermatocytes with an average number of CO-associated CDK2 foci of 16.12 and 17.5, respectively, excluding the sex body (n=25 for cHet; n=10 for Het) (Fig. 12B).

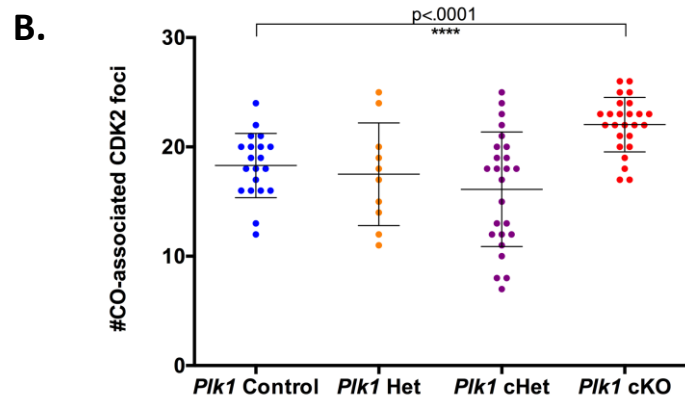
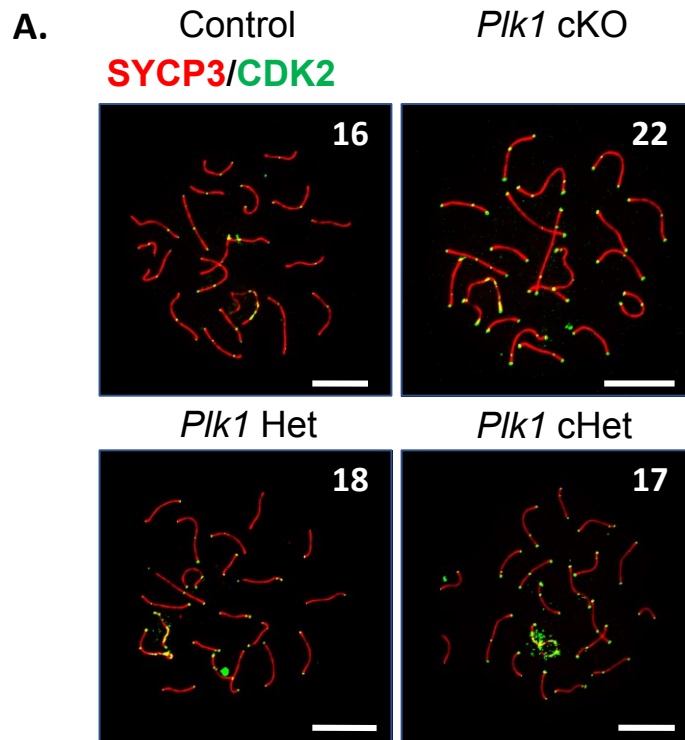


Fig 12. **A.** Representative spermatocyte chromosome spreads from mid-pachynema in control (*Plk1* +/Flo_x), Het (*Plk1* Flo_x/Del), cHet (*Plk1* +/Flo_x^{Sp_o11-Cre}), and cKO (*Plk1* Flo_x/Del^{Sp_o11-Cre}), stained for the indicated proteins and numbered by total CDK2 foci per nucleus (sex body excluded). Bar length: 10 μ m (x100 magnification). **B.** Quantification of CDK2 focus mid-pachynema in control (*Plk1* +/Flo_x), Het (*Plk1* Flo_x/Del), cHet (*Plk1* +/Flo_x^{Sp_o11-Cre}), and cKO (*Plk1* Flo_x/Del^{Sp_o11-Cre}). Each dot is count from a single nucleus (sex body excluded) from two pooled experiment. Bars, mean. P values were calculated by two-tailed Mann-Whitney test.

DISCUSSION

Previous studies in our lab elucidated the importance of PLK1-dependent phosphorylation in regulating SC disassembly during the metaphase transition (Jordan et al., 2012). In this study, we generated a germ-cell-specific conditional knockout mouse line for PLK1 to further elaborate its role during G2/M1 transition, with an emphasis on homologous recombination. Our results showed that adult *Plk1* cKO mice were infertile and had smaller testis. Our histological results showed that *Plk1* cKO cross-sections of seminiferous tubules displayed enlarged primary spermatocytes without the presence of any mature spermatids. TUNEL stained cross-sections of *Plk1* cKO testis demonstrated an increased number of apoptotic cells. The above data suggest that deletion of *Plk1* in mice leads to severe meiotic aberrancies. In addition, *Plk1* heterozygous mutant mice displayed reduced testis weight and increased TUNEL positive staining, indicating that PLK1 expression levels are also important during spermatogenesis.

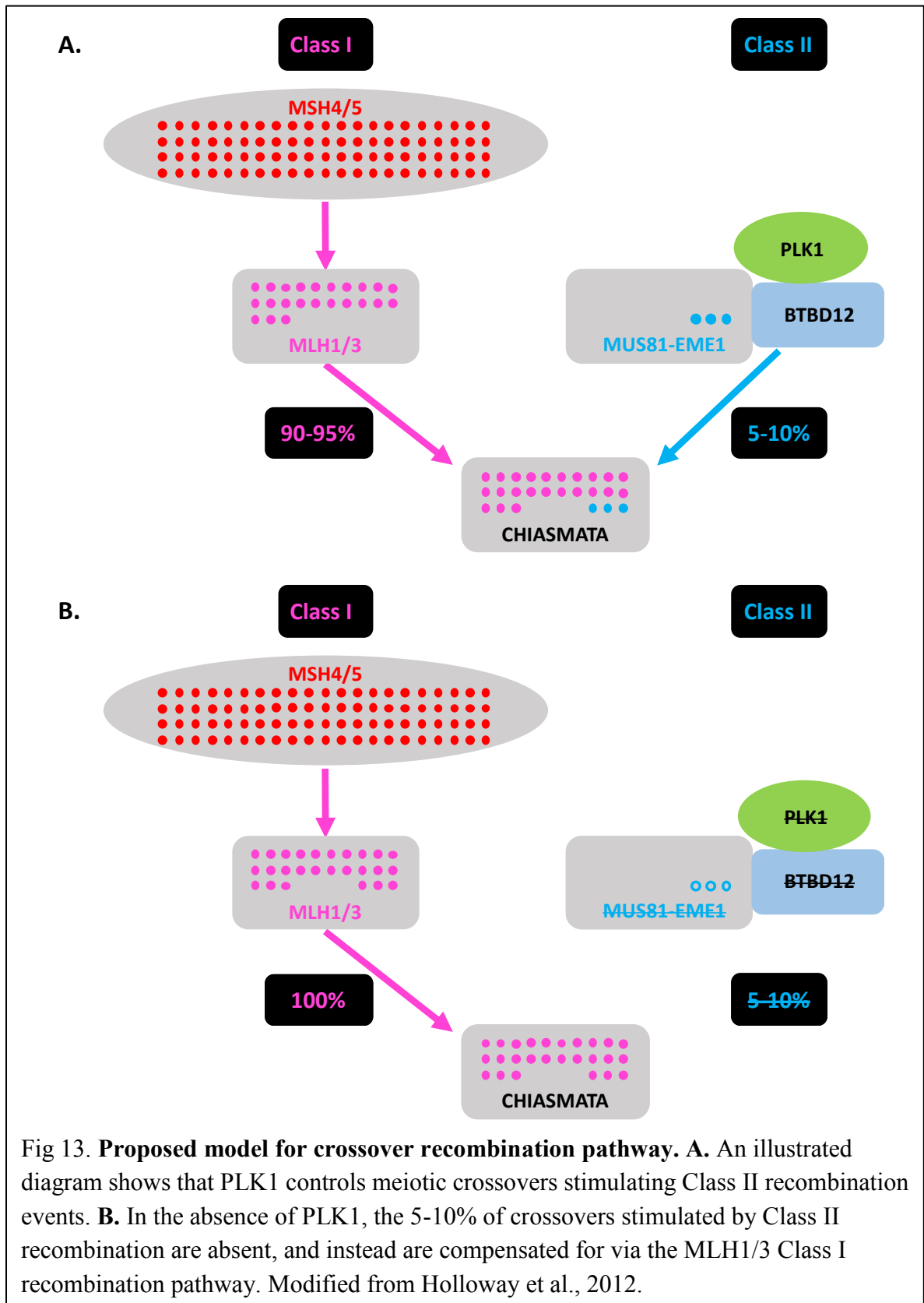
Homologous recombination (HR) is an essential DNA damage repair event to ensure proper segregation during meiosis (Hunter, 2015). We used spermatocyte chromatin spreads to assess foci numbers of various proteins that are required for HR. First, we showed that *Plk1* mutant spermatocytes displayed a reduction in RAD51 and DMC foci number. It is known that S14 of RAD51 is phosphorylated by PLK1 to trigger subsequent phosphorylation in human somatic cells (Yata et al., 2012). So, we speculate that the reduction in RAD51 foci number is caused by loss of PLK1-mediated phosphorylation on

RAD51 itself. Sequence alignment on RAD51 and DMC1 reveals remarkable similarity at the amino acid level (Masson and West, 2001). We therefore conjectured on the cause underlying reduction in DMC1 foci number by bridging what is known about RAD51. Computational predictions of kinase-specific phosphorylation sites show that S11 and S19 of DMC1 are candidates for PLK1-mediated phosphorylation, suggesting that PLK1 might regulate DMC1 in the same way it regulates RAD51 (Wong et al., 2007). Consequently, insufficient loading of RAD51 and DMC1 might be caused by a lack of PLK1-dependent phosphorylation on these proteins that is required to drive localization onto DNA damage sites. It's known that RAD51 and DMC1 have protein-protein interaction in mouse spermatocytes (Tarsounas et al., 1999). Disruption of PLK1 levels might delay the recruitment of RAD51 and therefore hinder the loading of its counterpart protein, DMC1. Interestingly, the extent of reduction in DMC1 foci number are the same among Het, cHet and cKO spermatocytes. Mutation of one allele of *Plk1* in Het and cHet spermatocytes is sufficient to display a meiotic defect as severe as mutation of both alleles in cKO spermatocytes, suggesting an obligatory role of PLK1 in regulating this early recombination intermediate. However, this haploinsufficiency did not affect RAD51 foci number, suggesting that PLK1 might have a different regulatory mechanism with DMC1.

Previous studies proposed a model for an increase in MLH1/3 foci number when the Class II MUS81-EME1 pathway is disrupted (Fig. 13) (Holloway et al., 2012). The Class I crossover pathway initiates with interference establishment by proteins like MSH4/5.

MLH1/3 selectively binds to these established sites, which ends with 90-95% of chiasmata. On the other hand, remaining chiasmata are generated by the alternative Class II MUS81-EME1 crossover pathway. It has been shown that in the absence of MUS81-EME1 or its interactive upstream protein BTBD12, there is an increase in MLH1/3 foci but unchanged chiasmata count (Holloway et al., 2012). It was proposed that loss of Class II MUS81-EME1 crossover pathway drives a complementary increase in Class I MLH1/3 events, regulated by several factors like BLM. In summary, the normal flux towards Class II events is lost. Instead, additional MLH1/3 foci are recruited to restore chiasmata counts. PLK1, as an interactive upstream protein, is known to phosphorylate MUS81-MMS4 to promote its nuclease activity in budding yeast (Gallo-Fernández et al., 2012). In mammalian systems, PLK1 is known to phosphorylate BTBD12 and then interact with the MUS81-EME1 complex (Wyatt et al., 2013). In our results, we showed that there was an 8.7% increase in MLH1 foci in cKO spermatocytes as compared to control spermatocytes. We propose that conditional knockout of *Plk1* blocks Class II events, which in turn triggers a shift towards Class I events. To demonstrate that Class I events increase, we analyzed an upstream protein of MLH1/3. CDK2 is a pro-crossover protein, selectively stabilizing recombination sites. By assessing crossover-associated CDK2 foci number, we showed that there was a 20.4% increase in cKO spermatocytes as compared to control spermatocytes. Our data further revealed that deletions of *Plk1* drive an increase in Class I MLH1/3 crossover formation.

In conclusion, our results revealed infertility and severe meiotic aberrancies in *Plk1* cKO spermatocytes. While initial events of HR appeared unchanged in *Plk1* mutant mice, alterations in RAD51, DMC1, MLH1, and CDK2 foci numbers suggested that PLK1 plays an important role in DNA repair during spermatogenesis. Interestingly, *Plk1* heterozygous mice displayed a phenotype as severe as *Plk1* cKO mice with regards to DMC1 foci number, suggesting a requirement for sufficient PLK1 levels during early meiotic recombination. Based on work conducted in budding yeast, further assessment of the MUS81-EME1 endonuclease will be crucial to further elucidate the mechanistic function of PLK1 during HR in spermatogenesis. A genetic screen will be performed to assess chiasmata count of mice with double mutations in *Plk1* and *Mlh3*. Continuing assessment of these defects will shed light on the many spatio-temporal roles of PLK1 during meiotic progression.



PUBLIC HEALTH RELEVANCE

Accurate execution of chromosome segregation during mitosis and meiosis maintains the generation of euploid daughter cells. Missegregation of chromosome causes aneuploidy, the leading cause of miscarriage, congenital birth defects and clinical disorders (Nagaoka et al., 2012). Down's syndrome is the most common trisomy disorder, predominantly originating from maternal nondisjunction of chromosome 21 (Hassold et al., 2007). It is reported that Down's syndrome happens in 1 of 750 live births, usually diagnosed with mental retardation (Orr et al., 2015). Although failure in maternal meiosis and increased maternal age are characterized as the main contributors to aneuploidy, spontaneous incidences of aneuploidy in spermatozoa cannot be neglected. Klinefelter syndrome (47, XXY), triple X syndrome (47, XXX) and Turner syndrome (45, X) are most commonly derived from paternal nondisjunction (Pacchierotti et al., 2007). Fluorescence in situ hybridization (FISH) analysis showed an estimated 1%-4% aneuploidy rate of sperm in healthy men (Templado et al., 2011). PLK1 has a crucial role in centrosome maturation, spindle assembly, metaphase transition (G2/M1) and cytokinesis (Petronczki et al., 2008). Inhibition of PLK1 in mouse oocytes has been reported to induce a meiotic arrest at G2/M1 transition and therefore cause infertility (Shen et al., 2010). Consequently, a molecular understanding of the factors that regulate chromosome dynamics during meiosis is necessary to better understand the cellular origins of these aneuploidy events or infertility.

PLK1, as a central cell cycle regulator for maintenance of genome integrity, has been reported to have an association with carcinogenesis and a potential in cancer therapy (Strebhardt et al., 2006). PLK1 are overexpressed in various types of human tumors, including breast cancer, prostate cancer, colorectal cancer (Strebhardt et al., 2006). Immunohistochemical analysis against PLK1 of thin malignant melanomas elucidated that elevated expression of PLK1 can act as a novel marker for metastasis (Kneisel et al., 2002). Treatment of cancer patients with PLK1 inhibitors is still under development. Since PLK1 is crucial for a series of events during cell cycle division, it is important to reach a balance between efficiency to suppress tumorigenesis and maintenance of normal cell growth.

REFERENCES

1. Anderson, L. K., Reeves, A., Webb, L. M., & Ashley, T. (1999). Distribution of crossing over on mouse synaptonemal complexes using immunofluorescent localization of MLH1 protein. *Genetics*, *151*(4), 1569-1579.
2. Archambault, V., & Carmena, M. (2012). Polo-like kinase-activating kinases: Aurora A, Aurora B and what else?. *Cell cycle*, *11*(8), 1490-1495.
3. Archambault, V., Lepine, G., & Kachaner, D. (2015). Understanding the polo kinase machine. *Oncogene*, *34*(37), 4799.
4. Bahassi, E. M., Conn, C. W., Myer, D. L., Hennigan, R. F., McGowan, C. H., Sanchez, Y., & Stambrook, P. J. (2002). Mammalian Polo-like kinase 3 (Plk3) is a multifunctional protein involved in stress response pathways. *Oncogene*, *21*(43), 6633.
5. Bellvé, A. R. (1993). [6] Purification, culture, and fractionation of spermatogenic cells. *Methods in enzymology*, *225*, 84-113.
6. Boddy, M. N., Gaillard, P. H. L., McDonald, W. H., Shanahan, P., Yates, J. R., & Russell, P. (2001). Mus81-Eme1 are essential components of a Holliday junction resolvase. *Cell*, *107*(4), 537-548.
7. Burkard, M. E., Randall, C. L., Larochelle, S., Zhang, C., Shokat, K. M., Fisher, R. P., & Jallepalli, P. V. (2007). Chemical genetics reveals the requirement for Polo-like kinase 1 activity in positioning RhoA and triggering cytokinesis in human cells. *Proceedings of the National Academy of Sciences*, *104*(11), 4383-4388.
8. Cahoon, C. K., & Hawley, R. S. (2016). Regulating the construction and demolition of the synaptonemal complex. *Nature Structural and Molecular Biology*, *23*(5), 369.
9. Cole, F., Kauppi, L., Lange, J., Roig, I., Wang, R., Keeney, S., & Jasin, M. (2012). Homeostatic control of recombination is implemented progressively in mouse meiosis. *Nature cell biology*, *14*(4), 424-430.
10. Costa, Y., & Cooke, H. J. (2007). Dissecting the mammalian synaptonemal complex using targeted mutations. *Chromosome Research*, *15*(5), 579-589.
11. Clyne, R. K., Katis, V. L., Jessop, L., Benjamin, K. R., Herskowitz, I., Lichten, M., & Nasmyth, K. (2003). Polo-like kinase Cdc5 promotes chiasmata formation and cosegregation of sister centromeres at meiosis I. *Nature Cell Biology*, *5*(5), 480.
12. de Cárcer, G., Manning, G., & Malumbres, M. (2011a). From Plk1 to Plk5: functional evolution of polo-like kinases. *Cell cycle*, *10*(14), 2255-2262.
13. de Cárcer, G., Escobar, B., Higuero, A. M., García, L., Ansón, A., Pérez, G., ... & Malumbres, M. (2011b). Plk5, a polo box domain-only protein with specific roles in neuron differentiation and glioblastoma suppression. *Molecular and cellular biology*, *31*(6), 1225-1239.

14. Elia, A. E., Cantley, L. C., & Yaffe, M. B. (2003). Proteomic screen finds pSer/pThr-binding domain localizing Plk1 to mitotic substrates. *Science*, 299(5610), 1228-1231.
15. Fraune, J., Schramm, S., Alsheimer, M., & Benavente, R. (2012). The mammalian synaptonemal complex: protein components, assembly and role in meiotic recombination. *Experimental cell research*, 318(12), 1340-1346.
16. Gallo-Fernández, M., Saugar, I., Ortiz-Bazán, M. Á., Vázquez, M. V., & Tercero, J. A. (2012). Cell cycle-dependent regulation of the nuclease activity of Mus81–Eme1/Mms4. *Nucleic acids research*, 40(17), 8325-8335.
17. Gómez R, Jordan PW, Viera A, Alsheimer M, Fukuda T, et al. (2013) Dynamic localization of SMC5/6 complex proteins during mammalian meiosis and mitosis implies functions in distinct chromosome processes. *J Cell Sci* 125: 5061– 5072.
18. Habedanck, R., Stierhof, Y. D., Wilkinson, C. J., & Nigg, E. A. (2005). The Polo kinase Plk4 functions in centriole duplication. *Nature cell biology*, 7(11), 1140.
19. Hanada, K., Budzowska, M., Modesti, M., Maas, A., Wyman, C., Essers, J., & Kanaar, R. (2006). The structure-specific endonuclease Mus81–Eme1 promotes conversion of interstrand DNA crosslinks into double-strands breaks. *The EMBO journal*, 25(20), 4921-4932.
20. Handel, M. A., & Schimenti, J. C. (2010). Genetics of mammalian meiosis: regulation, dynamics and impact on fertility. *Nature Reviews Genetics*, 11(2), 124-136.
21. Hartwell, L. H., Mortimer, R. K., Culotti, J., & Culotti, M. (1973). Genetic control of the cell division cycle in yeast: V. Genetic analysis of cdc mutants. *Genetics*, 74(2), 267-286.
22. Hassold, T., Hall, H., & Hunt, P. (2007). The origin of human aneuploidy: where we have been, where we are going. *Human molecular genetics*, 16(R2), R203-R208.
23. Hirose, Y., Suzuki, R., Ohba, T., Hinohara, Y., Matsuhara, H., Yoshida, M., ... & Yamamoto, A. (2011). Chiasmata promote monopolar attachment of sister chromatids and their co-segregation toward the proper pole during meiosis I. *PLoS genetics*, 7(3), e1001329.
24. Holloway, J. K., Booth, J., Edelmann, W., McGowan, C. H., & Cohen, P. E. (2008). MUS81 generates a subset of MLH1-MLH3-independent crossovers in mammalian meiosis. *PLoS genetics*, 4(9), e1000186.
25. Holloway, J. K., Mohan, S., Balmus, G., Sun, X., Modzelewski, A., Borst, P. L., ... & Cohen, P. E. (2011). Mammalian BTBD12 (SLX4) protects against genomic instability during mammalian spermatogenesis. *PLoS genetics*, 7(6), e1002094.

26. Hunter, N., & Kleckner, N. (2001). The single-end invasion: an asymmetric intermediate at the double-strand break to double-holliday junction transition of meiotic recombination. *Cell*, *106*(1), 59-70.
27. Hunter, N. (2015). Meiotic recombination: the essence of heredity. *Cold Spring Harbor perspectives in biology*, *7*(12), a016618.
28. Jordan PW, Karppinen J, Handel MA (2012) Polo-like kinase is required for synaptonemal complex disassembly and phosphorylation in mouse spermatocytes. *J Cell Sci* *125*: 5061–5072.
29. Kang, Y. H., Park, J. E., Yu, L. R., Soung, N. K., Yun, S. M., Bang, J. K., ... & Lee, K. S. (2006). Self-regulated Plk1 recruitment to kinetochores by the Plk1-PBIP1 interaction is critical for proper chromosome segregation. *Molecular cell*, *24*(3), 409-422.
30. Keeney, S., Giroux, C. N., & Kleckner, N. (1997). Meiosis-specific DNA double-strand breaks are catalyzed by Spo11, a member of a widely conserved protein family. *Cell*, *88*(3), 375-384.
31. Keeney, S. (2007). Spo11 and the formation of DNA double-strand breaks in meiosis. In *Recombination and meiosis* (pp. 81-123). Springer Berlin Heidelberg.
32. Kneisel, L., Strebhardt, K., Bernd, A., Wolter, M., Binder, A., & Kaufmann, R. (2002). Expression of polo-like kinase (PLK1) in thin melanomas: a novel marker of metastatic disease. *Journal of cutaneous pathology*, *29*(6), 354-358.
33. Kneitz, B., Cohen, P. E., Avdievich, E., Zhu, L., Kane, M. F., Hou, H., ... & Edelman, W. (2000). MutS homolog 4 localization to meiotic chromosomes is required for chromosome pairing during meiosis in male and female mice. *Genes & Development*, *14*(9), 1085-1097.
34. La Salle, S., Sun, F., & Handel, M. A. (2009). Isolation and short-term culture of mouse spermatocytes for analysis of meiosis. *Meiosis: Volume 2, Cytological Methods*, 279-297.
35. Lee, K. S., Grenfell, T. Z., Yarm, F. R., & Erikson, R. L. (1998). Mutation of the polo-box disrupts localization and mitotic functions of the mammalian polo kinase Plk. *Proceedings of the National Academy of Sciences*, *95*(16), 9301-9306.
36. Lipkin, S. M., Moens, P. B., Wang, V., Lenzi, M., Shanmugarajah, D., Gilgeous, A., ... & Schwartzberg, P. (2002). Meiotic arrest and aneuploidy in MLH3-deficient mice. *Nature genetics*, *31*(4), 385-390.
37. Masson, J. Y., & West, S. C. (2001). The Rad51 and Dmc1 recombinases: a non-identical twin relationship. *Trends in biochemical sciences*, *26*(2), 131-136.
38. Matthew, E., & El-Deiry, W. (2007). Replication stress, defective S-phase checkpoint and increased cell death in Plk2-deficient human cancer cells.
39. McMahill, M. S., Sham, C. W., & Bishop, D. K. (2007). Synthesis-dependent strand annealing in meiosis. *PLoS biology*, *5*(11), e299.

40. Nagaoka, S. I., Hassold, T. J., & Hunt, P. A. (2012). Human aneuploidy: mechanisms and new insights into an age-old problem. *Nature Reviews Genetics*, *13*(7), 493.
41. Orr, B., Godek, K. M., & Compton, D. (2015). Aneuploidy. *Current Biology*, *25*(13), R538-R542.
42. Park, J. E., Soung, N. K., Johmura, Y., Kang, Y. H., Liao, C., Lee, K. H., ... & Lee, K. S. (2010). Polo-box domain: a versatile mediator of polo-like kinase function. *Cellular and Molecular Life Sciences*, *67*(12), 1957-1970.
43. Pacchierotti, F., Adler, I. D., Eichenlaub-Ritter, U., & Mailhes, J. B. (2007). Gender effects on the incidence of aneuploidy in mammalian germ cells. *Environmental research*, *104*(1), 46-69.
44. Petronczki, M., Lénárt, P., & Peters, J. M. (2008). Polo on the rise—from mitotic entry to cytokinesis with Plk1. *Developmental cell*, *14*(5), 646-659.
45. Reynolds, A., Qiao, H., Yang, Y., Chen, J. K., Jackson, N., Biswas, K., ... & Höög, C. (2013). RNF212 is a dosage-sensitive regulator of crossing-over during mammalian meiosis. *Nature genetics*, *45*(3), 269-278.
46. Roeder, G. S. (1997). Meiotic chromosomes: it takes two to tango. *Genes & development*, *11*(20), 2600-2621.
47. Santucci-darmanin, S., Walpita, D., Lespinasse, F., Desnuelle, C., Ashley, T., & Paquis-flucklinger, V. (2000). MSH4 acts in conjunction with MLH1 during mammalian meiosis. *The FASEB Journal*, *14*(11), 1539-1547.
48. Sansam, C. L., & Pezza, R. J. (2015). Connecting by breaking and repairing: mechanisms of DNA strand exchange in meiotic recombination. *The FEBS journal*, *282*(13), 2444-2457.
49. Seki, A., Coppinger, J. A., Jang, C. Y., Yates, J. R., & Fang, G. (2008). Bora and the kinase Aurora a cooperatively activate the kinase Plk1 and control mitotic entry. *Science*, *320*(5883), 1655-1658.
50. Sourirajan, A., & Lichten, M. (2008). Polo-like kinase Cdc5 drives exit from pachytene during budding yeast meiosis. *Genes & development*, *22*(19), 2627-2632.
51. Stanzione, M., Baumann, M., Papanikos, F., Dereli, I., Lange, J., Ramlal, A., ... & Jasin, M. (2016). Meiotic DNA break formation requires the unsynapsed chromosome axis-binding protein IHO1 (CCDC36) in mice. *Nature cell biology*.
52. Steegmaier, M., Hoffmann, M., Baum, A., Lénárt, P., Petronczki, M., Krššák, M., ... & Grauert, M. (2007). BI 2536, a potent and selective inhibitor of polo-like kinase 1, inhibits tumor growth in vivo. *Current biology*, *17*(4), 316-322.
53. Strebhardt, K., & Ullrich, A. (2006). Targeting polo-like kinase 1 for cancer therapy. *Nature reviews cancer*, *6*(4), 321.

54. Sunkel, C. E., & Glover, D. M. (1988). polo, a mitotic mutant of *Drosophila* displaying abnormal spindle poles. *Journal of cell science*, 89(1), 25-38.
55. Svendsen, J. M., Smogorzewska, A., Sowa, M. E., O'Connell, B. C., Gygi, S. P., Elledge, S. J., & Harper, J. W. (2009). Mammalian BTBD12/SLX4 assembles a Holliday junction resolvase and is required for DNA repair. *Cell*, 138(1), 63-77.
56. Szostak, J. W., Orr-Weaver, T. L., Rothstein, R. J., & Stahl, F. W. (1983). The double-strand-break repair model for recombination. *Cell*, 33(1), 25-35.
57. Tarsounas, M., Morita, T., Pearlman, R. E., & Moens, P. B. (1999). RAD51 and DMC1 form mixed complexes associated with mouse meiotic chromosome cores and synaptonemal complexes. *The Journal of cell biology*, 147(2), 207-220.
58. Templado, C., Vidal, F., & Estop, A. (2011). Aneuploidy in human spermatozoa. *Cytogenetic and genome research*, 133(2-4), 91-99.
59. Watanabe, Y., & Nurse, P. (1999). Cohesin Rec8 is required for reductional chromosome segregation at meiosis. *Nature*, 400(6743), 461-464.
60. Ward, J. O., Reinholdt, L. G., Motley, W. W., Niswander, L. M., Deacon, D. C., Griffin, L. B., ... & Eppig, J. J. (2007). Mutation in mouse hei10, an e3 ubiquitin ligase, disrupts meiotic crossing over. *PLoS genetics*, 3(8), e139.
61. Wong, Y. H., Lee, T. Y., Liang, H. K., Huang, C. M., Wang, T. Y., Yang, Y. H., ... & Hwang, J. K. (2007). KinasePhos 2.0: a web server for identifying protein kinase-specific phosphorylation sites based on sequences and coupling patterns. *Nucleic acids research*, 35(suppl_2), W588-W594.
62. Wu, Z. Q., & Liu, X. (2008). Role for Plk1 phosphorylation of Hbo1 in regulation of replication licensing. *Proceedings of the National Academy of Sciences*, 105(6), 1919-1924.
63. Wyatt, H. D., Sarbajna, S., Matos, J., & West, S. C. (2013). Coordinated actions of SLX1-SLX4 and MUS81-EME1 for Holliday junction resolution in human cells. *Molecular cell*, 52(2), 234-247.
64. Yata, K., Lloyd, J., Maslen, S., Bleuyard, J. Y., Skehel, M., Smerdon, S. J., & Esashi, F. (2012). Plk1 and CK2 act in concert to regulate Rad51 during DNA double strand break repair. *Molecular cell*, 45(3), 371-383.
65. Zickler, D., & Kleckner, N. (1999). Meiotic chromosomes: integrating structure and function. *Annual review of genetics*, 33(1), 603-754.

CURRICULUM VITAE

Xueqi ZHAO

xzhao42@jhu.edu • 608-886-6748 • 929 N Wolfe St Apt 520, Baltimore, MD, 21205

PERSONAL DATA

Date of birth: November 14, 1993

Place of birth: Chengdu, Sichuan, China

EDUCATION

09/16-present **Johns Hopkins Bloomberg School of Public Health**

ScM in Biochemistry and Molecular Biology

ScM thesis: The Role of Polo-like Kinase 1 (PLK1) in Homologous Recombination during Mammalian Spermatogenesis

MHS thesis: DNA Damage Response in Embryonic Stem Cells vs. Differentiated Cells

09/12-12/15 **University of Wisconsin-Madison, Dept. of Biochemistry**

B.S. in Biochemistry, expected in Dec.2015, Certificate in Environment Studies

Thesis: Examination of Wild Type HCA II (Human Carbonic Anhydrase II) & Y7F

EXPERIENCE

11/16-present **The Jordan Lab in Johns Hopkins Univ.**

--Graduate Research Assistant, Dr. Philip Jordan

Importance of structural maintenance of chromosomes complexes and cell cycle kinases in regulating DNA repair, chromosome segregation and meiosis

01/16-05/16 **Chengdu Ishine Biotechnology Inc.**

--Research and Development Staff

Development of in vitro diagnosis products for cardiovascular disease

09/15-12/15 **The Ntambi Lab in Univ. of Wisconsin-Madison**

--Undergraduate Research Assistant, Dr. James M. Ntambi

Role of stearyl-CoA denaturase in metabolism and its genetic regulation

06/15-07/15 **Center of Growth, Metabolism and Aging, Sichuan Univ.**

--Summer Research Assistant, Dr. Zhixiong Xiao

Signaling pathway in cellular senescence and major proteins such as p63 in regulation of cancer cell migration

10/13-12/13 **The Raines Lab in Univ. of Wisconsin-Madison**

--Undergraduate Research Assistant, Dr. Ronald T. Raines

Relationship between amino-acid sequence and protein function, and to the creation of novel molecules with desired properties